Waikato Regional Council Technical Report 2015/26

An assessment of the impacts of climate change in the Waikato region: Applying CMIP5 data

www.waikatoregion.govt.nz
ISSN 2230-4355 (Print)
ISSN 2230-4363 (Online)

Prepared by:
Drs Meng Wang, Yinpeng Li and Chonghua Yin

For:
Waikato Regional Council
Private Bag 3038
Waikato Mail Centre
HAMILTON 3240

24 June 2015

Document #: 3433696

Approved for release by:
Dominique Noiton

Date November 2015

Disclaimer

An Assessment of the Impacts of Climate Change in the Waikato Region: Applying CMIP5 Data

September 2014

CLIMsystems Ltd

Drs Meng Wang, Yinpeng Li and Chonghua Yin

Reviewed by Dr Peter Urich

Executive Summary

Climate change is projected to alter long-term average climatic conditions and climatic variability in New Zealand. The best estimates are for a temperature increase of 0.2–2.0°C by 2040 and 0.7–5.1°C by 2090, with marked seasonal changes in rainfall and extreme events (Ministry for the Environment, 2008 (based on CMIP3 data). This report provides a broad technical assessment of the physical effects of climate change in the Waikato region. Projections cover short (2030), medium (2070) and long-term (2100) timeframes. Ensembles (or parallel scenarios) of up to 40 CMIP5 Global Climate Models (GCMs) were used to generate the future scenarios. Eight climatic indices were used to represent the major climate change-induced effects, including mean temperature, mean precipitation, extreme precipitation change, peak streamflow change, Potential Evapotranspiration Deficit (PED), Temperature-Humidity Index (THI), Growing Degree Days (GDD), and extreme wind.

Baseline and future scenarios for the climate change-related indices exhibit both spatial and temporal variability across the region. The projections indicate that mean annual temperature could increase by 1.17 (0.95-1.33)°C by 2070 and by 1.25 (1.00-1.45)°C by 2100. Summer annual mean temperature could increase with the highest seasonal change: 1.23 (0.95-1.43)°C by 2070 and up to 1.27 (1.00-1.50)°C by 2100.

Mean annual precipitation change is highly variable both annually and seasonally, ranging between a decrease of 4.56% and an increase of 9.22% by 2070; and between a decrease of 4.84% and an increase of 9.90% by 2100. The increase in precipitation is the highest (up to 4.6%) in autumn, by 2070, in the northern part of Thames-Coromandel, Waitomo, Otorohanga and Taupo districts. The largest decrease in precipitation is projected to occur in the Thames-Coromandel districts with up to 2.7% decrease in spring. The highest mean precipitation changes are projected for the Waitomo, Otorohanga, South Waikato and Taupo districts.

Extreme daily precipitation changes indicate an increase that is consistently located in north-east parts of the Waikato region – i.e., in the Hauraki and Thames-Coromandel districts and the north part of the Waikato district.

Peak streamflow changes are expected to increase in rivers such as the Kauaeranga and Waihou rivers which were selected for further analysis on the basis that extreme precipitation increases were projected to be highest in the areas through which these rivers flow. The Average Recurrence Intervals (ARIs) for peak streamflows are also expected to decrease (i.e. peak streamflows of specific values occur more frequently).

Projections for changes in Potential Evapotranspiration Deficit, PED, used as an indicator for drought, also highlight the spatial variability of impacts with the highest PED values (where PED>400mm) located in the Hauraki and Matamata-Piako districts by 2100. However, PED>200mm projections are more widespread across the Waikato region by 2070 and 2100, particularly in the central, northern and eastern parts. Drought-related stress on agricultural production systems and ecosystems in the Waikato region is therefore an issue that regional resource management will need to address into the future, in order to identify and assess feasible adaptation options that will ameliorate projected impacts.

The Temperature-Humidity Index, THI, indicates that mildly stress-inducing conditions (THI>72) for animals such as dairy cows are widespread across the Waikato region by 2070 and 2100.

Moderately stress-inducing conditions (THI>78) are more restricted to the central parts of the Waikato region by 2070 and 2100, with two 'hotspots' evident in the Hauraki and Matamata-Piako districts and further south in the Otorohanga district, particularly by 2100.

Growing Degree Days, GDD, projections indicate that a lengthening of the growing season is expected across the entire Waikato region, although the increase is spatially variable and highest in northern districts where temperatures are warmer and lowest in the Taupo district. This projected lengthening of the growing season is likely to have beneficial effects on pasture and crop productivity, and may create opportunities for new commercial crops to be cultivated. The increase in GDD also may have an impact on native species or species of importance to biosecurity, where GDD changes are likely to induce more favourable growing conditions.

The hot spots for extreme wind events are in the Thames-Coromandel, Waitomo, Otorohanga, Rotorua and Taupo districts. The extreme wind speed is projected to change but in small magnitudes in this century.

The uncertainties associated with the future projections of the nine climatic indices used in this assessment increase progressively between 2030 and 2100 scenarios, including uncertainties associated with future GHG concentration profiles, the earth's climate sensitivity to the GHG emissions, and the extent of the effects of feedback mechanisms that may influence the rate and magnitude of climate change. The uncertainty has been represented in this assessment by illustrating the spread of individual GCM projections within the various ensemble results.

The new projections with the new AR5 data are similar to the previous results in AR4, except PED and sea level rise. The reasons may be: 1) the radiative forcing of RCPs scenarios are different from SRES scenarios, 2) more GCMs employed in AR5 ensemble. The warming trend in Waikato is smaller than AR4 and the decrease in precipitation projection is also milder, so the PED change scarcely in the median scenario. The improvement in modelling land-ice contributions to sea level rise produced much higher projections of global sea level rise and this is reflected in sea level rise scenarios for the Waikato's coastal areas.

Based on the findings of this Assessment, we provide recommendations for more in-depth impact assessments that will inform adaptation strategies and processes for the Waikato region. Following from this, it should be possible to identify a range of indicators and adaptation options needed to respond to the projected future effects of climate change in the Waikato region.

[Note: Detailed analyses of bio-physical impacts, risks and specific adaptation strategies for human, managed or natural systems in the region are not a part of this report. These would include impacts that affect the Regional Council's core functions and responsibilities of natural hazard management (floods, droughts and storm damage, in particular), biodiversity and biosecurity management, and coastal area management, water and land management and regional planning among others. In addition, climate change has implications for regional agricultural productivity, and infrastructure that require more detailed assessments].

Table of Contents

List of Figures

List of Tables

Glossary

(Adapted from the IPCC (2013) and IPCC (2010) Working Group I and Working Group II Reports)

Adaptation: An adjustment that is planned or unplanned (autonomous) within human and natural systems, in response to climatic impacts that are either experienced in the present or anticipated in the future. The adjustment is expected to reduce harmful impacts or make use of the beneficial opportunities that the climatic impacts present.

Baseline: A reference period of time against which future change is measured. The baseline may refer to climatic or non-climatic conditions and can represent an historical baseline (e.g. 1986-2005), a current baseline (including observable present-day conditions), or a future baseline (that excludes that driver factor of interest). Therefore, multiple baselines are possible, depending on how they are defined.

Climate sensitivity: The amount of global temperature rise that would occur (to a new equilibrium), when the concentration of atmospheric carbon dioxide is doubled above pre-industrial levels. In climate impact assessments, the climate sensitivity can be represented as Low, Medium or High, when generating future climate projections.

Ensemble: A group of climate simulations from multiple climate models, used to generate future climate projections. The variations across the different simulations in the ensemble, represented by a range, are also an estimate of the uncertainty associated with the future projections. Ensembles can be made with multiple climate models (to test climate model differences) or by varying the initial conditions for a single climate model (to test internal climate variability).

General Circulation Models (GCMs) (or Global Climate Models): A numerical representation of the global climate system based on the physical, chemical and biological properties of its components, their interactions and feedback processes, and accounting for all or some of its known properties. Models of varying complexity are in use. Coupled Atmosphere-Ocean General Circulation Models (AOGCMs) provide a representation of the climate system that is near the most comprehensive end of the spectrum currently available. Climate models are applied as a research tool to study and simulate the climate, and for operational purposes, they include monthly, seasonal and inter-annual climate predictions.

Impacts: The manifested effects of climate change on natural and human systems. 'Potential' impacts refer to the total impacts that are likely to occur for a given projection of climate change, while 'residual' impacts are the impacts after taking into account the effect of adaptation measures, to reduce harm or exploit benefits of a projected climate change.

Impact assessment: A technical process that identifies and evaluates the effects of climate change on natural and human systems and that may include monetary and/or non-monetary terms. The assessment typically involves the selection of relevant climatic indices that the system under consideration is sensitive to. More detailed assessments integrate non-climatic variables (and scenarios), as well as more detailed quantitative modelling and/or qualitative information to assess changes to one or more systems.

Pattern scaling: A technique used to compare equilibrium experiments from global climate models (GCMs). The GCM patterns are then combined with simple climate model simulations to generate scenarios of regional climate change for a range of radiative forcing scenarios, for which GCM runs are not available (as it is a resource intensive process to generate a single

GCM run). Pattern scaling generates accurate estimates of regional climate changes that would be simulated by a GCM under different radiative forcings (Mitchell, 2001).

Projection: A possible future evolution of a measurable variable that is typically computed with the aid of a model. Projections are different to predictions since they are subject to inherent uncertainty associated with underlying assumptions about socio-economic and technological developments at global and regional scales in the future, for instance, which are not fully known at the present time.

Scenario: A plausible, though often simplified narrative, storyline or description of how the future may develop. This narrative is based on assumptions about driving forces of change and the key relationships, and which must be internally consistent with one another. Future projections can be used to develop these scenarios in addition to other information.

Vulnerability: A measure of the degree to which a natural or human system is unable to cope with the projected adverse impacts of climate variability and change. It is a function of the magnitude and rate of climate change, as well as other factors that influence the sensitivity or exposure of the systems, as well as their capacity to adapt to the anticipated changes.

1 Introduction

Climate change will modify average climate and climate variability, thereby modifying the frequency and intensity of existing risks and hazards, as well as introducing some long-term shifts in climate regimes across New Zealand (MfE, 2008; IPCC, 2014). Local government agencies are responsible for a range of functions that may be affected by climate change, under the Local Government Act 2002, and the Resource Management Act 1991. For regional councils, these functions may include management of regional water, and land resources, biosecurity, natural hazards management, emergency management, and regional land transport. Local authorities own community assets that may be vulnerable to climate change effects (MfE, 2008).

Based on this recognition, the Waikato Regional Council requested a strategic assessment of the impacts of climate change on the Waikato region, provided in this Assessment. The results are intended to show the broad patterns of change for the region both in terms of projections of spatially-explicit climate changes and climate variability and extremes. They are also intended to provide strategic information that is relevant to planning adaptation strategies for the region. Nine climatic variables are included in this regional assessment as follows (illustrated in Figure 1):

1. Mean temperature change (Section 2.1)
2. Mean precipitation change (Section 2.1)
3. Extreme precipitation change (Section 2.2)
4. Peak stream flow change (Section 2.3)
5. Potential Evapotranspiration Deficit (PED) (Section 2.4)
6. Temperature-Humidity Index (THI) (Section 2.5)
7. Growing Degree Days (GDD) (Section 2.6)
8. Sea level rise (Section 2.7)
9. Extreme wind (Section 2.8)

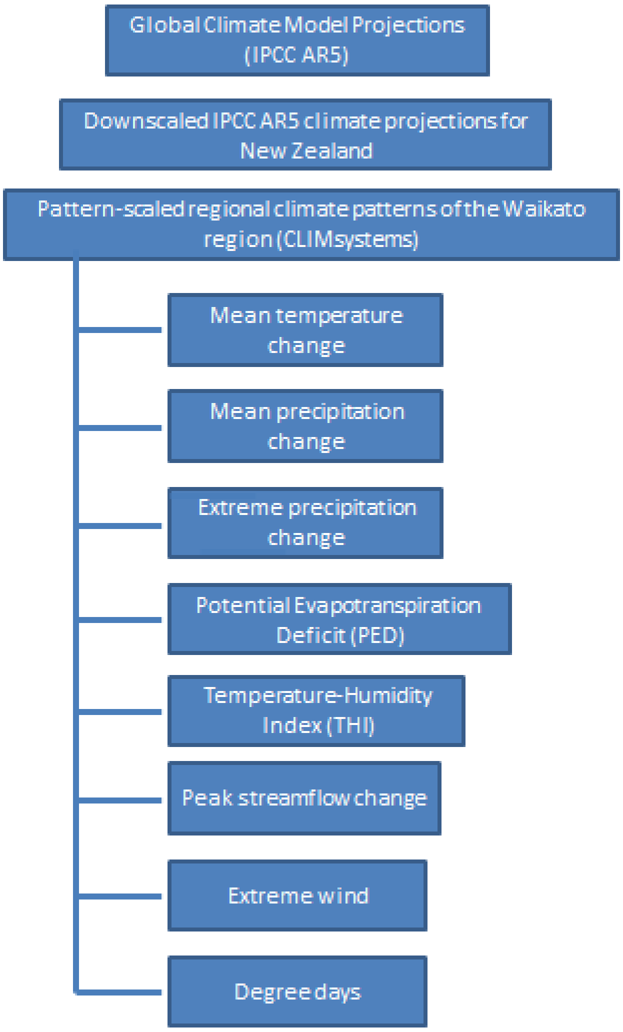

Figure 1 Climate change patterns for the regional climate change assessment in Waikato.

These variables are important indices for assessing the climate–induced impacts to regional agricultural productivity, livestock stress, flood and drought-induced hazards and coastal inundation and erosion that are important to medium and long-term resource planning and management. However, to characterize the risks to specific systems (such as an agricultural production landscape, or a coastal area), it will be necessary to conduct more detailed localized assessments, for example, using risk-based modelling approaches, which are beyond the scope of the present study (key recommendations for such analyses are provided at the end of the Assessment). The data and methodologies used to produce each of the nine climate variables are described in the respective Sections 2.1-2.8

In terms of its climate, the Waikato region is relatively sheltered by high elevation areas, which result in the predominantly cool winters with frosts and warm, dry and settled summers. Hence, the region experiences less wind than other parts of the country. Rainfall is highest in the western and eastern ranges and the Coromandel peninsula and lowest in the central Waikato basin (Kenny et al., 2001), and is influenced by the orography and prevailing wind patterns.

The Waikato region experiences less extreme climatic variations than other parts of New Zealand – particularly with respect to droughts and floods. However, over the last two decades, with the onset of more intensive dairy farming and higher stocking rates of cows, there has been a greater perception of drought risk, even in years that would otherwise be considered climatically moderate (Kenny et al., 2001). This context of dependence on agricultural production increases the climate-induced vulnerability of the region into the future.

The 12 Territorial Authority boundaries in the Waikato region are shown in Figure 2, to assist with interpreting the spatial climate scenarios produced in this Assessment.

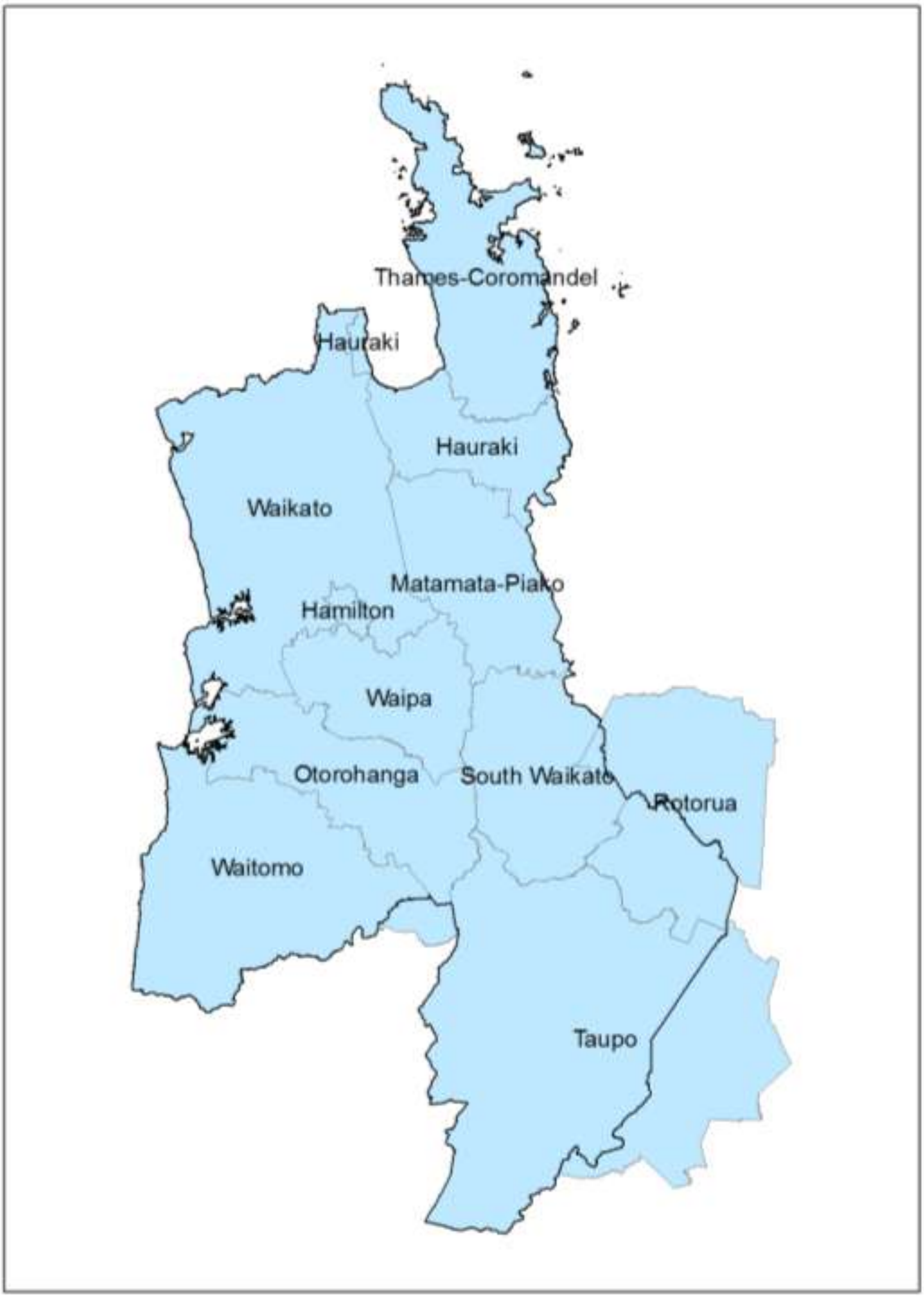

Figure 2 The Waikato region with its 11 Districts and City boundaries (excluding marine boundaries).

2 Baseline and future climate in the Waikato region

To produce the baseline and future climate projections for the Waikato region several important considerations need to be made, as they relate to assessing the impacts, risks and adaptation to climate change (Jones, 2010; and Benestad, 2002):

1. The spatial scale at which climate information is provided, to assess risks and appropriate adaptation actions;
2. There is a need for regionalised projections of climate change;
3. Local climates may exhibit gradual trends and non-linear changes in response to global warming which are usually not resolved in General Circulation Models (GCMs).

The climate change scenarios produced in this Assessment are based on global General Circulation Model (GCM) outputs.

We implemented a technique called **pattern scaling** to produce climate patterns for global coverage (0.5°*0.5°) (see Appendix 1 for a full description of this method), and then regrid to 100m resolution for Waikato region. Pattern scaling has a higher degree of confidence for temperature-related impacts, while less confidence for precipitation-related impacts of climate change can be expected. This is because attributes of climate variability and anthropogenic change are often unresolved due to large variability in precipitation patterns. As a result, systems affected by multiple variables including extreme climatic variables (for instance, agricultural cropping systems, livestock production systems and natural ecosystems), usually face higher uncertainty with respect to climate change related impacts.

Ensembles (or parallel scenarios) of up to **40** Global Climate Models (GCMs)[1] were used to generate the future scenarios, by providing the range of ensemble member values per variable. The spatial scenarios and statistics produced are presented using **ensemble statistics**, that is, the Low (25th percentile), Median (50th percentile), and High (75th percentile) values of the ensemble. (Please note: in this Assessment, all references **to Low (25th), Median (50th) and High (75th) percentiles** of the ensemble results will be given as 'Low', 'Median' and 'High' respectively). 40 GCMs included in IPCC AR5 (CMIP5) were employed for the ensemble. Details of the GCMs used for producing the future scenarios of specific variables are provided in Appendices 3-6.

The following steps were undertaken to produce the results contained in this Assessment (and further details of the steps are provided in Appendix 1):

1. Temperature and precipitation patterns were normalised, using the global mean temperature change of the corresponding period and GCM; and

2. Spatial and statistical analyses were undertaken based on the ensemble results, for: (a) the Baseline period (1976-2008, from observed climate data from NIWA), and (b) three future time periods: 2030, 2070 and 2100, for the different variables.

[1] Each GCM result is referred to as an ensemble 'member'.

To generate the future climate scenarios, the Representative Concentration Pathways (RCPs) from IPCC Fifth Assessment Report (IPCC AR5, 2010) were used. The RCPs are four greenhouse gas concentration (not emissions) trajectories adopted by the IPCC for its Fifth Assessment Report (AR5). The four RCPs, **RCP2.6, RCP4.5, RCP6.0, and RCP8.5**, are named after a possible range of radiative forcing values in the year 2100 (of 2.6, 4.5, 6.0, and 8.5 W/m^2, respectively) (Table 1).

Table 1 Overview of Representative Concentration Pathways (RCPs)

	Description[2]	**CO_2 Equivalent**	**SRES Equivalent**	**Publication – IA Model**
RCP8.5	Rising radiative forcing pathway leading to 8.5 W/m^2 in 2100.	1370	A1FI	Raiahi *et al.* 2007 – MESSAGE
RCP6.0	Stabilization without overshoot pathway to 6 W/m^2 at 2100	850	B2	Fujino *et al.*; Hijioka *et al.* 2008 – AIM
RCP4.5	Stabilization without overshoot pathway to 4.5 W/m^2 2100	650	B1	Clark *et al.* 2006; Smith and Wigley 2006; Wise *et al.* 2009 – GCAM
RCP2.6	Peak in radiative forcing at about 3 W/m^2 before 2100 and decline	490	None	van Vuuren *et al.*, 2007; van Vuuren *et al.* 2006 - IMAGE

Figure 3 shows the global mean temperature change projected for four RCP scenarios, between 1995 and 2100. Global mean temperature change projected ranges from 0.73°C (RCP2.6) to 0.96° (RCP8.5) by 2030, and by 2100, between 0.9°C under RCP2.6 and 4.09°C under RCP8.5 (Table 2).

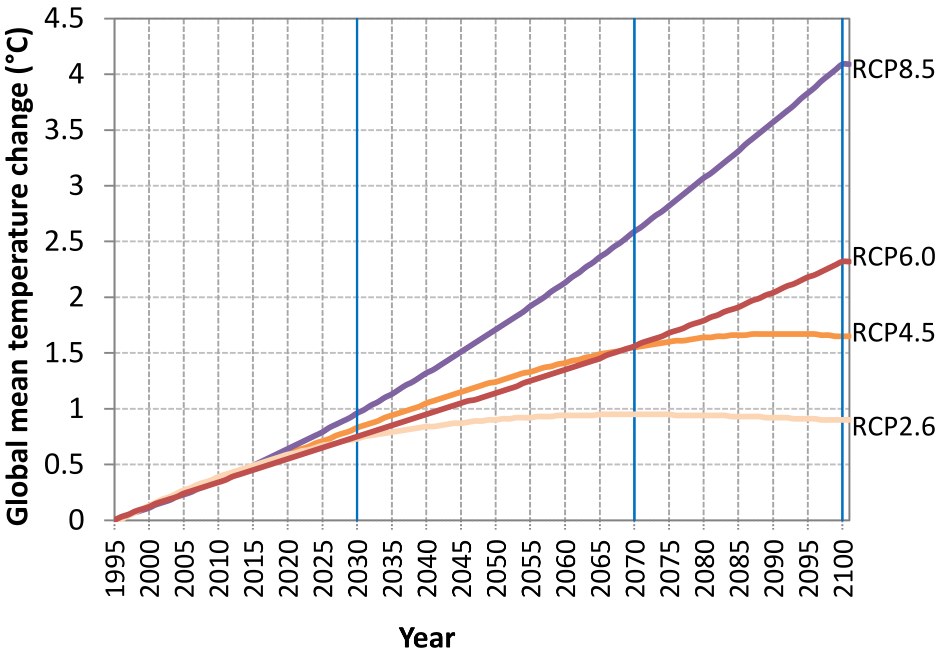

Figure 3 The global mean temperature change of the three selected RCP scenarios. The graph shows that up to 2030, global mean temperature is projected to increase by about 1.0°C, irrespective of the RCP scenario and subsequently the future temperature change projections diverge by 2070 and even more by 2100, depending on the RCP scenario.

[2] Approximate radiative forcing levels were defined as ±5% of the stated level in W/m^2 relative to pre-industrial levels. Radiative forcing values include the net effect of all anthropogenic GHGs and other forcing agents.

Table 2 Global annual mean temperature change (°C) in the selected scenarios and times slices.

GMT change (°C)	2030	2070	2100
RCP2.6	0.73	0.95	0.9
RCP4.5	0.83	1.55	1.65
RCP6.0	0.75	1.56	2.32
RCP8.5	0.96	2.59	4.09

In comparison with the previous assessment in 2010, three points need to be addressed:

1. The scenarios, GCM ensemble and percentiles selected in this report are totally different from the previous report.
2. The chosen time periods also change in this report.
3. Only the median projections in 2100 under RCP4.5 and RCP 8.5 may be comparable with the previous median projections in 2100 under B1 and A1FI.

The following Sections 2.1-2.8 provide the baseline and future scenarios of 10 climate variables selected for this regional assessment in Waikato.

2.1 Mean temperature and precipitation change

2.1.1 Introduction

Mean temperature and precipitation changes are two fundamental and widely measured climate variables, from which various other climate-related variables are derived. Temperature changes are one of the most easily measured changes in climate, while precipitation measurements are more difficult, often due to the influence of local wind patterns of measurement gauges (IPCC, 2013). Changes in mean temperature and precipitation can have direct and indirect impacts on natural and human systems, depending on the direction and magnitude of the change, and the sensitivity of those systems to the resultant climate changes (Thuiller et al., 2005; Patz et al., 2005). Seasonal variations in mean temperature and precipitation influence evapotranspiration rates and soil water content, plant photosynthetic activity, metabolic processes of plants and animals, (Dai et al., 2004; Root et al., 2003; and Woodward, 1987), and stream-water flows (Brito-Castillo et al., 2003) to name a few.

2.1.2 Methodology and data

Mean temperature and precipitation were derived using the pattern scaling method described in Appendix 1. The climate data used to generate the baseline climate were provided by NIWA (as gridded climate data) for the period 1976-2008. The **40 GCMs** selected for generating the future climate change scenarios are listed in Appendix 3.

2.1.3 Results

The **normalized annual mean temperature change patterns** (Figure 4), per degree global warming for the Waikato region indicates that annual mean temperature change is 0.72-0.77°C (Median) per degree global warming. Therefore, annual mean temperature changes at a lower rate in the Waikato region compared to the global scale. Even at the High (75th percentile) of mean temperature change, the temperature increase is still lower than global mean temperature increase. Compared to results in the previous assessment, the projections of warming based on IPCC AR5 data (obtained from new RCP scenarios and 40 GCMs outputs) are just slightly higher than the previous results from 12 GCMs output SRES scenarios in IPCC AR4.

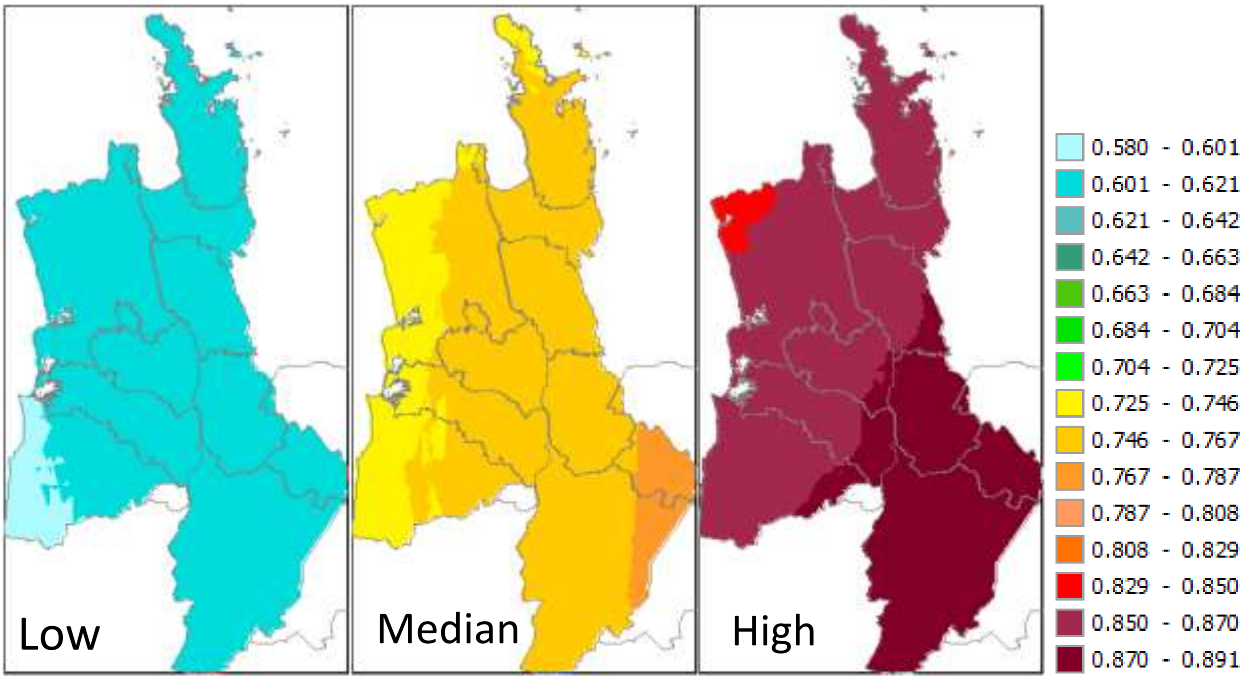

Figure 4 The normalized annual mean temperature change patterns (˚C per degree global mean temperature increase): using the 40-GCM ensemble for Low (25th), Median (50th), and High (75th) percentiles.

2.1.3.1 Baseline and future mean annual and seasonal temperature

Using the baseline climate data and normalized change patterns, it is possible to produce the future projections for any RCP scenario and time periods. To produce the patterns in Figure 5, only the Median ensemble values of the 2070 scenarios were used.

Annual mean temperature is projected to increase by 1.17 (0.95-1.33) °C by 2070 (RCP4.5) and by 1.25 (1.00-1.45) °C by 2100 (RCP4.5) (Table 3). Under the high scenario, RCP8.5, the temperature increases by 3.02 (2.50, 3.51) ˚C by 2100 for the Waikato region. This projection is lower than the previous result (3.37˚C) under the highest SRES emission scenario, A1FI.

The summer (DJF) and autumn (MAM) mean temperature increases faster than for the other seasons with median change of 1.23°C in DJF and 1.22 °C in MAM by 2070 (RCP4.5) and by up to 1.27 (1.00-1.50) °C by 2100 (RCP4.5). Winter (JJA) mean temperature increases by 1.16 (0.90-1.28) ˚C by 2070 (RCP4.5) and up to 1.24 (0.98-1.42) ˚C by 2100 (RCP4.5). Spring (SON) is still the slowest temperature increase among the seasons. It is noted that the autumn mean temperature increase is projected as much as summer under the RCP 4.5 (Figure 6, RCP4.5 MAM), especially in Rotorua and Western Taupo even increasing faster than summer (Figure 5, RCP4.5 MAM).

Table 3 Mean seasonal and annual temperature changes (°C): RCP4.5 and RCP8.5 using Low, Median, and High percentiles of the ensemble, for 2030, 2070 and 2100. DJF, December-January-February; MAM, March-April-May; JJA, June-July-August; SON, September-October-November; ANN, Annual mean.

		RCP4.5			RCP8.5		
		Low	**Median**	**High**	**Low**	**Median**	**High**
	2030	0.50	0.64	0.75	0.59	0.75	0.88
DJF	2070	0.95	**1.23**	1.43	1.57	2.00	2.38
	2100	1.00	**1.27**	1.50	2.50	**3.25**	3.73
	2030	0.54	0.64	0.75	0.62	0.75	0.88
MAM	2070	1.00	**1.22**	1.46	1.72	2.01	2.45
	2100	1.07	**1.27**	1.50	2.62	**3.20**	3.88
	2030	0.49	0.62	0.71	0.58	0.72	0.83
JJA	2070	0.90	**1.16**	1.28	1.50	1.96	2.15
	2100	0.98	**1.24**	1.42	2.45	**3.00**	3.47
	2030	0.49	0.59	0.64	0.56	0.66	0.75
SON	2070	0.89	1.08	1.23	1.50	1.80	2.00
	2100	0.98	1.17	1.27	2.42	2.92	3.24
	2030	0.50	0.62	0.73	0.59	0.73	0.84
ANN	2070	0.95	**1.17**	1.33	1.55	1.97	2.28
	2100	1.00	**1.25**	1.45	2.50	**3.02**	3.51

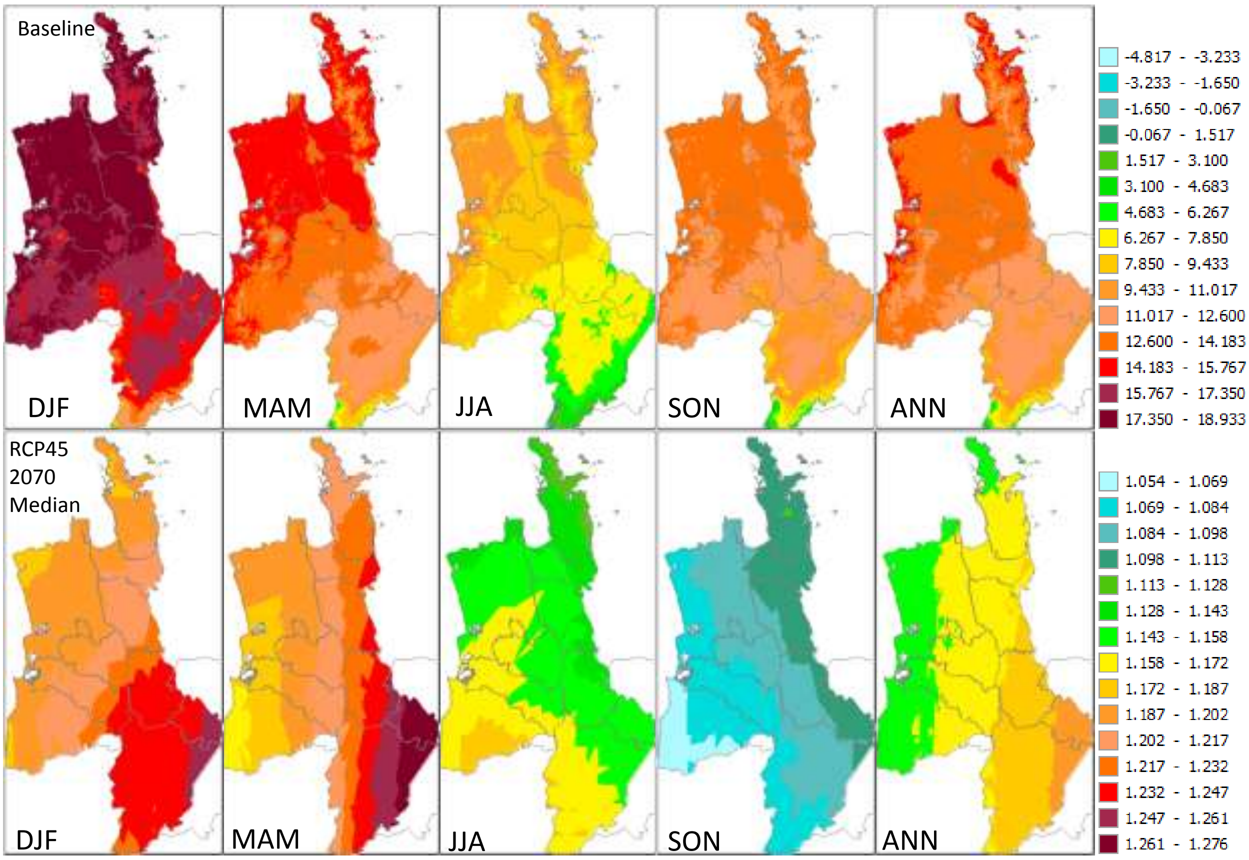

Figure 5 Mean seasonal and annual temperature change (°C) by 2070 (RCP4.5-Median): Baseline (top panel) and change by 2070 (RCO4.5, Median)

The spatial patterns of warming using AR5 data are different from the projections obtained from AR4 data. The temperature increases faster in the western than the eastern of Waikato under RCPs all through all seasons, except winter. The maximum increase is located in Rototua and the western parts of Taupo.

Seasonal and annual mean temperature changes are shown in Figure 6. The size of the boxes indicates the spread of the modelled values by each of the 40 GCMs in the ensemble and is also a measure of the uncertainty associated with the projections at each time period, such that larger boxes indicate higher associated uncertainty among GCMs, typical of scenarios for 2100.

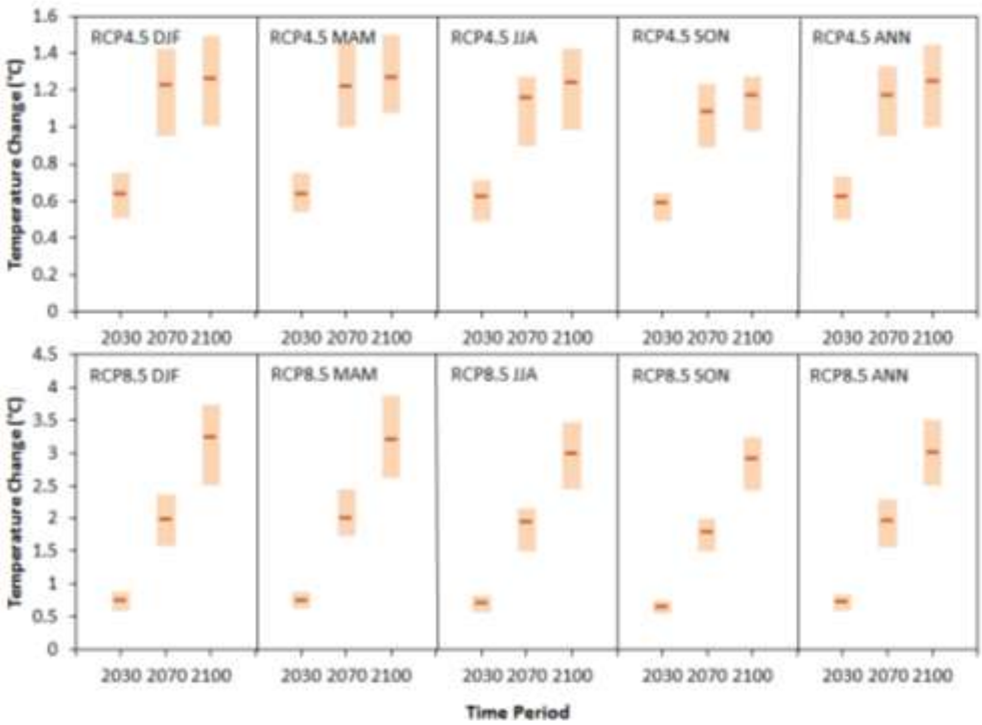

Figure 6 Statistics on the mean seasonal and annual temperature changes: RCP4.5 (top) and RCP8.5 (bottom panel), for 2030, 2070, and 2100. DJF, December-January-February; MAM, March-April-May; JJA, June-July-August; SON, September-October-November; ANN, Annual mean. The bottom and top of box are the low and high percentiles, and the mark in box shows the median projection of 40 GCMs.

2.1.3.2 Baseline and future precipitation projections

The **normalized annual mean precipitation change patterns** in the Waikato region, show variability that is characteristic of precipitation projections, which are largely dependent on whether the projected westerly winds show an increase or a decrease across New Zealand (MfE, 2008).

Figure 7 shows that annual mean precipitation change is projected to be between a 0.56% to 1.82% increase in precipitation (Median), per degree global warming. To put the variability of the precipitation projections in context, the Low 25th percentile shows a decrease of 2.49-3.53% and the High 75th percentile shows an increase of 5.04-6.69%. Therefore, mean annual precipitation changes are projected to be relatively low, using the 40 GCM ensemble.

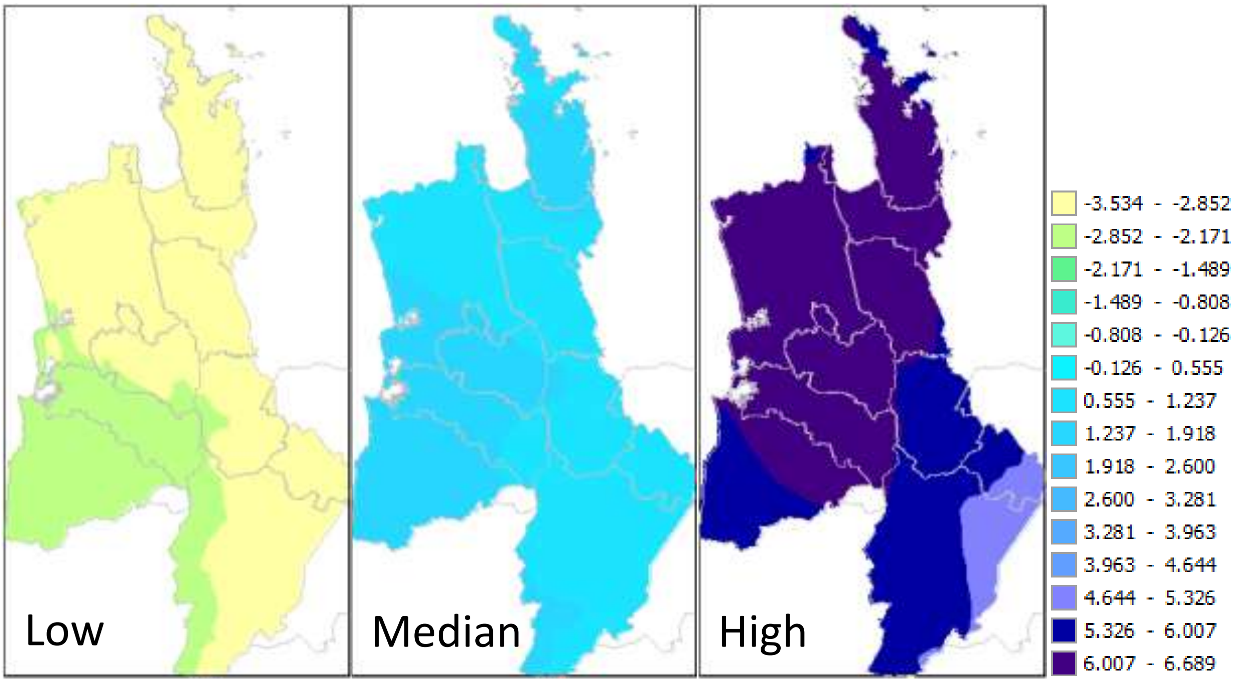

Figure 7 The normalized mean annual precipitation change (percent per degree global warming). Patterns show the Low, Median, and High of the 40-GCM ensemble.

The **annual mean monthly precipitation changes** project both increases and decreases that are spatially variable. Annual mean precipitation shows a minimal increase of 1.87 (-4.56, 9.22) % by 2070 and 1.99 (-4.84, 9.90) % increase by 2100 under RCP4.5, though the range of values indicate both significant increases and decreases (Table 4). The low Median precipitation values therefore should be interpreted in the context of the inherent variability that is evident in the precipitation projections. The new projections of median precipitation change (e.g. 1.99% under RCP4.5 and 4.92% under RCP8.5 in 2100) using AR5 data increase much higher than the previous values (e.g. 0.31% under B1 and 0.72% under A1FI in 2100).

Seasonal mean precipitation changes include projections for winter (JJA) mean precipitation increasing the most with up to 1.54 (-4.22, 8.23)% increase by 2070 (RCP4.5) and 1.64 (-4.49, 8.77) % increase by 2100 (RCP4.5). Summer (DJF) mean precipitation is projected to increase by 2.71 (-4.70, 10.71) % by 2070 (RCP4.5) and by 2.89 (-5.02, 11.54) % by 2100 (RCP4.5). The maximum increase in precipitation happens in autumn, and the worst decrease occurs in spring.

Table 4 Seasonal and annual mean precipitation changes (% change to baseline): 2030, 2070 and 2100 scenarios using RCP4.5 and RCP8.5, Low, Median, and High percentiles of the 40-GCM ensemble. DJF, December-January-February; MAM, March-April-May; JJA, June-July-August; SON, September-October-November; ANN, Annual mean.

		RCP4.5			RCP8.5		
		Low	Median	High	Low	Median	High
	2030	-2.53	1.46	5.81	-2.91	1.67	6.68
DJF	2070	-4.70	**2.71**	10.71	-7.86	4.54	18.10
	2100	-5.02	**2.89**	11.54	-12.48	7.17	28.69
	2030	-1.19	2.33	6.86	-1.38	2.69	7.99
MAM	2070	-2.22	4.36	12.81	-3.72	7.28	21.41
	2100	-2.36	4.63	13.63	-5.86	11.48	34.00
	2030	-2.26	0.83	4.42	-2.61	0.96	5.09
JJA	2070	-4.22	**1.54**	8.23	-7.04	2.57	13.76
	2100	-4.49	**1.64**	8.77	-11.11	4.07	21.78
	2030	-3.75	-0.60	2.82	-4.33	-0.70	3.25
SON	2070	-7.03	-1.12	5.27	-11.74	-1.88	8.79
	2100	-7.45	-1.20	5.60	-18.65	-2.96	13.92
	2030	-2.43	1.00	4.98	-2.81	1.16	5.73
ANN	2070	-4.56	**1.87**	9.22	-7.63	3.12	15.57
	2100	-4.84	**1.99**	9.90	-11.96	**4.93**	24.54

Figure 8 shows that the whole area of Waikato is projected to experience increases in annual mean precipitation, which is totally different from the previous results. In terms of seasonal patterns, summer (DJF) mean precipitation increase is highest in the northern costal parts of Waikato mainly located in the Thames-Coromandel district. Only the precipitation in spring (SON) is projected to decrease. The largest decrease is in the northern point of Thames-Coromandel and the western areas of Rotorua.

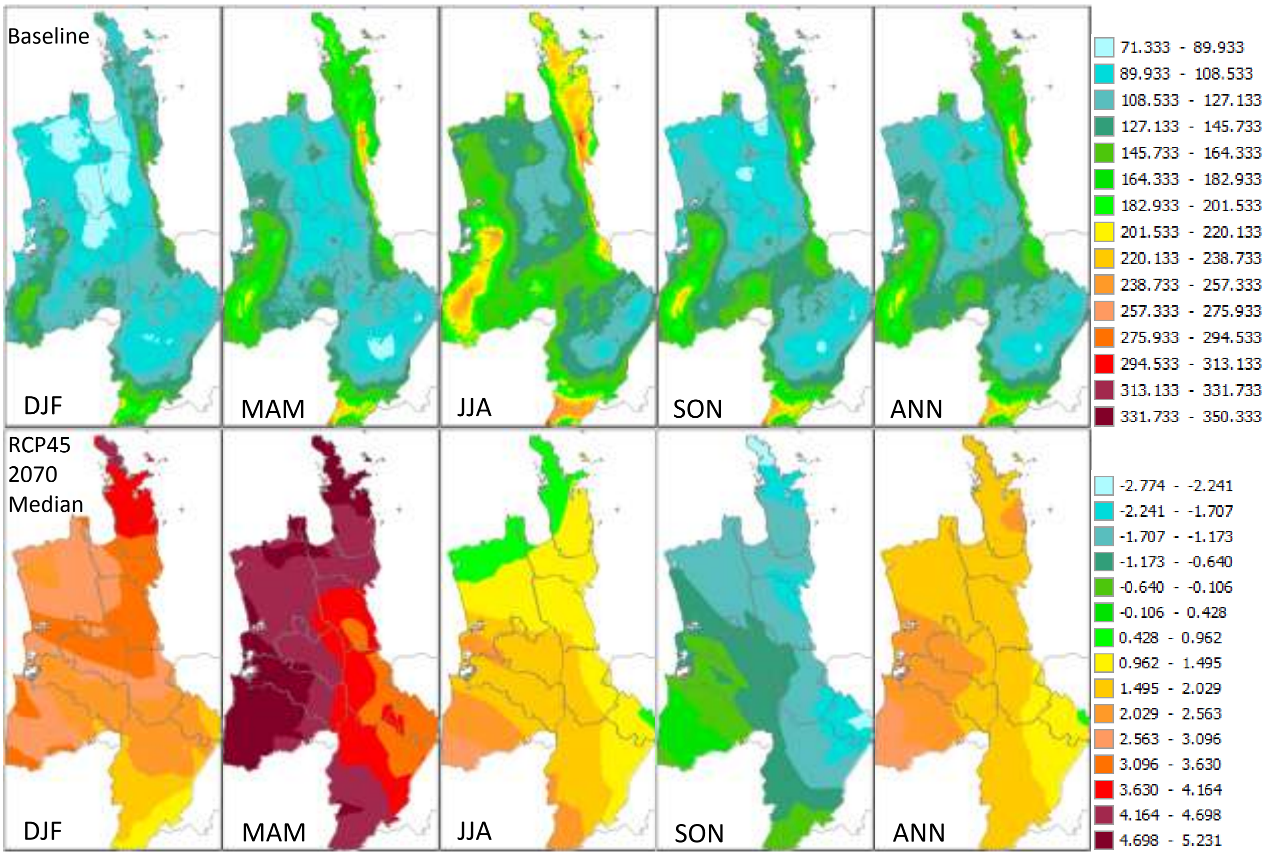

Figure 8 Mean seasonal and annual precipitation changes: Baseline (top panel) and 2070 scenario (RCP4.5-Median) (bottom panel). DJF, December-January-February; MAM, March-April-May; JJA, June-July-August; SON, September-October-November; ANN, Annual mean.

Mean monthly precipitation change in the Waikato region is relatively small for 2030, while it is characterized by a large spread among GCMs in 2070 and 2100 (indicated by the larger blue boxes in Figure 9. There is an evident change in median change value between 2030 and after 2070. These variations are the result of different GCM model projections of mean precipitation change for each time period and season. They also indicate that uncertainty associated with the future projections and is the highest for 2100 scenarios and in highest for the summer (DJF) of the 2100 (RCP8.5) scenarios.

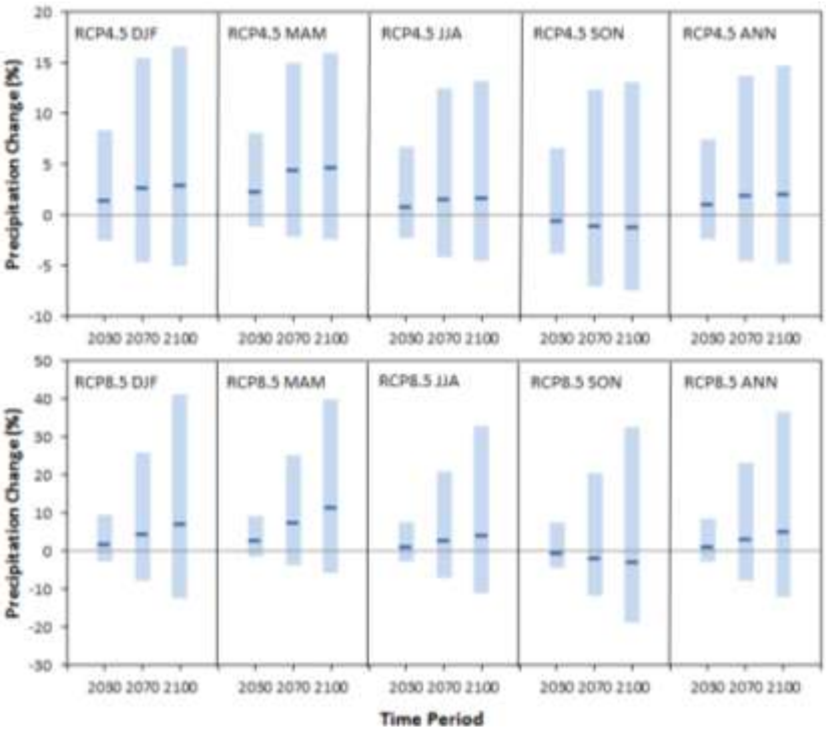

Figure 9 Statistics of mean monthly precipitation change: 40-GCM ensemble range illustrated by the blue boxes, rcp4.5 (top panel) and RCP8.5 (bottom panel) scenarios. DJF, December-January-February; MAM, March-April-May; JJA, June-July-August; SON, September-October-November; ANN, Annual mean. The bottom and top of box are the low and high percentiles, and the mark in box shows the median projection of 40 GCMs.

2.1.4 Discussion and conclusion

The projected changes in mean annual temperature relative to the baseline period of 1976-2008, are consistent with our earlier assessment. By 2070, annual mean temperature is projected to increase by 1.17 (0.95-1.33) °C, and by 1.25 (1.00-1.45) °C by 2100 (Table 2). Mean annual precipitation changes both in magnitude and direction, although changes are relatively small and exhibit more spatial variability than mean annual temperature over the region. On the other hand, it should be noted that precipitation extremes, are projected to change more markedly, and will be addressed in Section 2.2 of this Assessment. The magnitude of the change for both mean annual temperature and precipitation is dependent on the emissions scenario for the future.

When results are aggregated between RCP4.5 and RCP8.5 for the 2070 scenarios (Table 3), mean seasonal and annual temperature changes are: 1.23 (0.95, 1.43) °C in Summer, 1.22 (1.00, 1.46) °C in Autumn, 1.16 (0.90, 1.28) °C in Winter, 1.08 (0.89, 1.23) °C in Spring, and 1.17 (0.95, 1.33) °C for the Annual mean by 2070. These results for 2070 and 2100 are comparable with those of the Ministry for the Environment (MfE, 2008, pgs. 16 and 17); however, the time scales and GHG scenarios used are not exactly the same and may explain why our results report slightly higher change values. MfE (2008) used 2040 (2030–2049) and 2090 (2080–2099), while we have used 2070 and 2100, respectively. The projected increase in temperature using IPCC AR5 data is slightly lower than the previous projections using AR4.

The projected changes in mean seasonal and annual precipitation change, relative to the baseline period (1976-2008), when aggregated between RCP4.5 and RCP8.5 for the 2070 scenarios (Table 4) are: 2.71 (-4.70, 10.71) % in Summer, 4.36 (-2.22, 12.81) % in Autumn, 1.54 (-4.22, 8.23) % in Winter, -1.12 (-7.03, 5.27) % in Spring, and 1.87 (-4.56, 9.22) % for the Annual mean by 2070. By comparison with MfE (2008, pg. 24), this report shows higher change values for mean seasonal precipitation projections, and this may be due to the selection of different GHG scenarios between the two studies. Using AR5 data, the increases in seasonal and mean precipitation are projected to be significantly higher, and the decreases are much smaller than the previous projections derived from AR4 data.

There are variations in the direction of change in projected mean seasonal and annual precipitation change (projections for both increases and decreases). Therefore, it is recommended that Council needs to assess areas where decreases are projected, and how these are spatially connected to areas where increases are projected, particularly through increased river and stream flow volumes in headwaters (MfE, 2008).

2.2 Extreme precipitation change

2.2.1 Introduction

Precipitation extremes refer to extreme high or low precipitation events over time and are linked to flood and drought-related events (Sansom and Renwick, 2007). As a result, these extremes have attracted considerable research focus due to the potential hazards these present to human and natural systems. Extreme precipitation events are projected to increase with climate change, even in areas where the total precipitation is projected to decrease (Meehl et al., 2007), since global warming will noticeably enhance the hydrological cycle at both global and local scales. In most mid to high latitude and tropical areas, precipitation extremes are expected to increase more than mean precipitation, as is also projected for New Zealand (MfE, 2010; Meehl et al., 2007).

2.2.2 Methodology and data

In order to assess adequately the climate change impact on extreme precipitation events, the characteristics of GCM-simulated precipitation and its relationship to global warming need to be evaluated (Perkins et al. 2007; Alexandra and Arblaster 2008). Additionally, the evaluation of observed and modelled trends has shown that the confidence in GCM projected extremes of precipitation is much less than that of temperature (e.g. Kharin et al. 2007, Kiktev et al. 2007).

In general, the magnitude of changes in precipitation extremes simulated by GCMs is found to have a linear relationship with the strength of GHG emissions or is in proportion to the global warming trend (Alexander and Arblaster 2009, Tebaldi et al. 2006), which corresponds with the linear response theory of pattern scaling. For the extreme precipitation change analysis undertaken in this assessment, Appendix 3 provides further details of the methodology implemented and lists the **22 GCMs** used to produce the ensemble projections.

2.2.3 Results

The **normalized changes to extreme daily precipitation** (percentage changes) relative to the baseline period are shown in Table 5, for Average Recurrence Intervals (ARIs) ranging between 5-300 years. The extreme daily precipitation changes between 4.01% (for a 5-year ARI) and 6.94% (for a 300-year ARI) (Median), and a 100-year ARI is projected to change by 6.05%.

(Note: the percent change in extreme daily precipitation under the Low and High percentiles of the 22-GCM ensemble also should be considered in assessing the changes for each ARI).

The median increase in extreme precipitation using AR5 data is projected to reduce by half of the previous results for all ARIs.

Table 5 Normalised extreme daily precipitation changes (%). The average Recurrence Intervals (ARI) tested range from 5 to 300 years, for Low, Median and High percentiles of the 22-GCM ensemble.

ARI (year)		5	10	15	20	30	40	50	100	150	200	300
Low	%	2.51	2.48	2.80	2.80	2.80	2.82	2.88	3.34	3.66	3.83	4.07
Median	%	4.01	4.47	4.99	5.21	5.36	5.44	5.50	6.05	6.26	6.43	6.94
High	%	4.96	5.62	6.56	6.85	7.97	8.54	8.94	10.47	11.22	11.65	13.00

The **extreme precipitation intensity** for an event with a 20-year ARI changes from a maximum of ca 302.0mm/day (baseline) up to a maximum of ca 328.1mm/day by 2100 (RCP4.5); for a 50-year ARI changes from ca 389.6mm/day (baseline) to 428.4mm/day by 2100 (RCP4.5); and a 100-year event changes from a maximum of ca 486.5mm/day (baseline) up to a maximum of 517.3mm/day by 2100 (RCP4.5) (Figure 10). The baseline values (from 1976-2008) in this report are slightly different from the previous report (from 1972-2008).

The most extreme daily precipitation values are consistently located in the north-eastern parts of the Waikato region – in the Hauraki district, and north into the Thames-Coromandel district, and north parts of the Waikato district, particularly by 2070 and 2100. Similar as in the previous AR4 assessment, Thames-Coromandel, in particular, shows consistently higher values spatially distributed across the whole district – a pattern that is not evident anywhere else in the Waikato region, and could be associated with the relatively small and steep catchments that characterise the district.

Future projections under all scenarios tested indicate that extreme daily precipitation change values will increase. This is despite mean annual and seasonal precipitation scenarios showing both positive and negative changes that are spatially variable (refer to Figures 8 and 9 and Table 5).

The range of values projected by the different GCMs varies more widely by 2100 (illustrated by the size of the green bars in Figure 11) which is a measure of the spread and uncertainty associated with the projections by the 22-GCM model simulations by this time period.

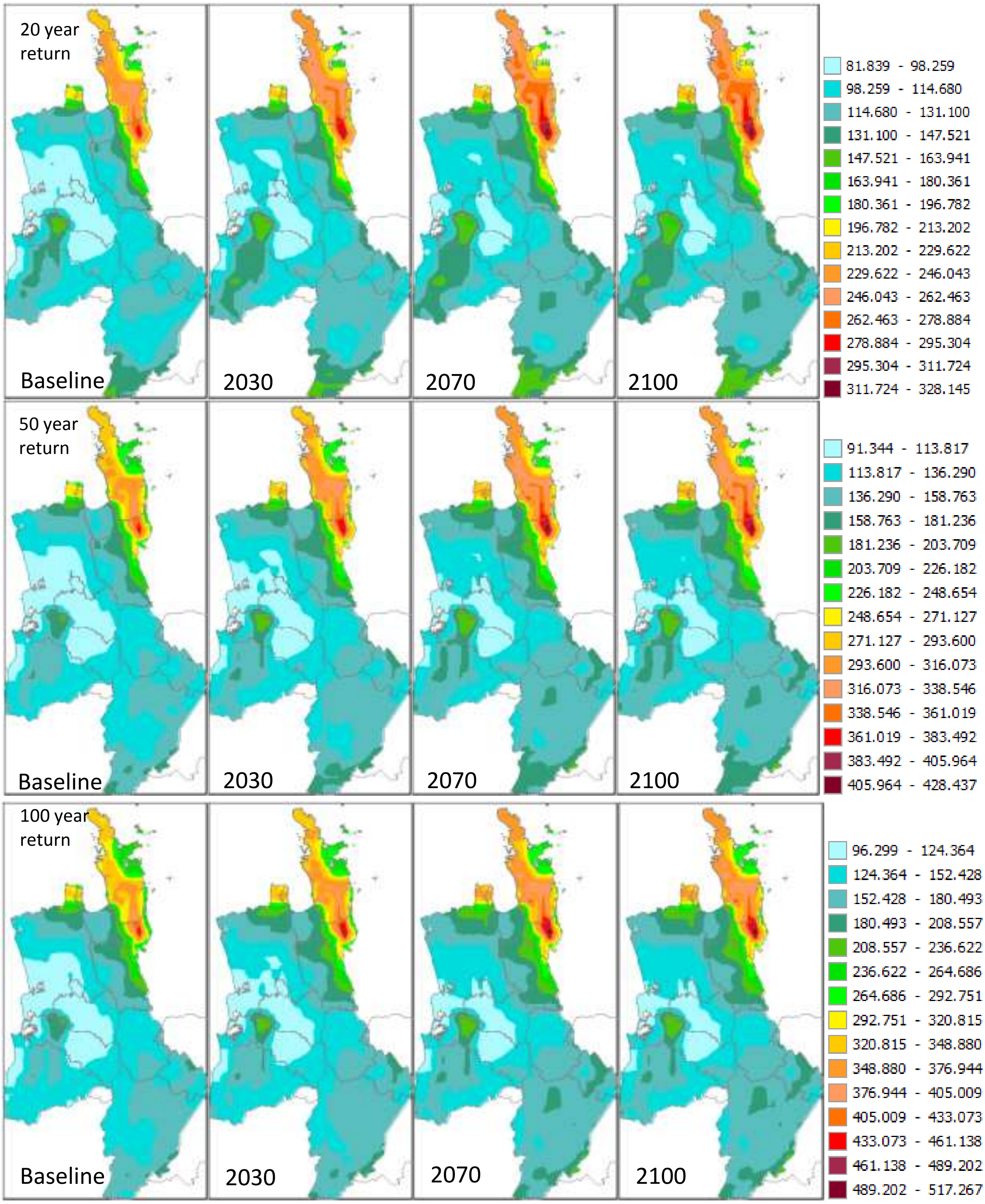

Figure 10 Extreme daily precipitation intensity (mm/day): Baseline and median projections for 20-year, 50-year and 100-year ARIs, for 2030, 2070, and 2100 (RCP4.5, Median) scenarios.

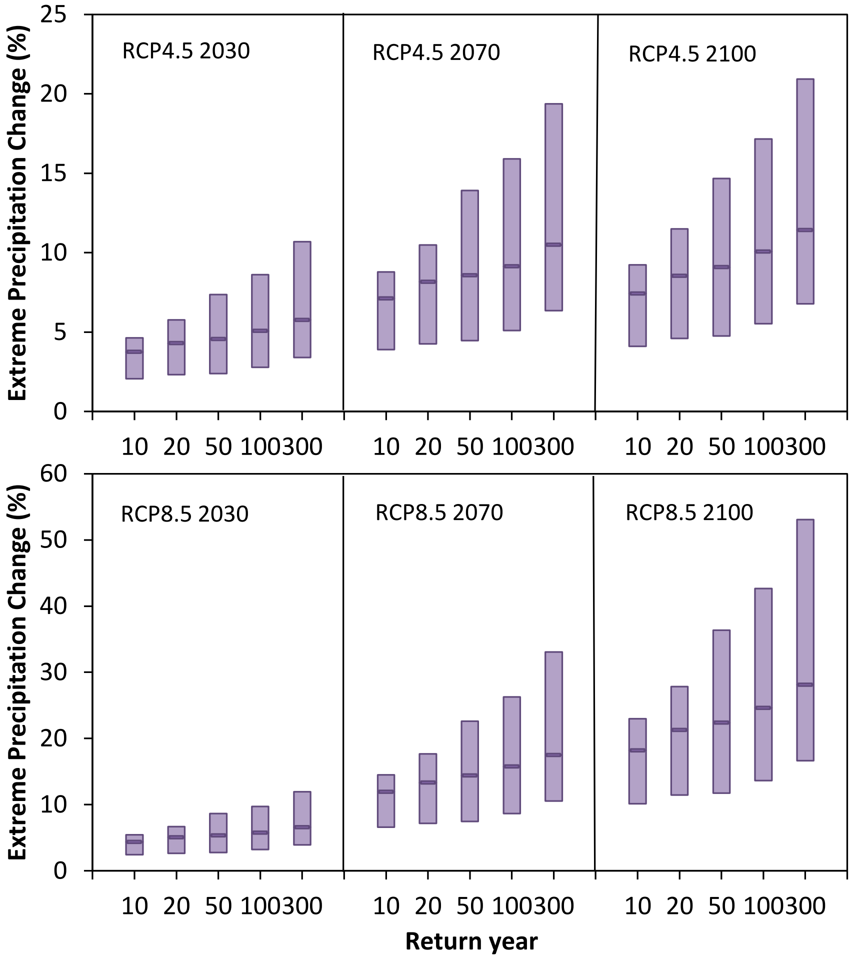

Figure 11 Extreme daily precipitation changes (percent change) for the Waikato region: RCP4.5 (top panel) and RCP8.5 (bottom panel), for 2030, 2070 and 2100 scenarios. Results from the 22-GCM ensemble, Low, Median and High percentiles represented by the purple boxes and marks: the bottom and top of box are the low and high percentiles, and the mark in box shows the median projection of 22 GCMs.

Table 6 shows results of the analysis of extreme precipitation changes by 2070 (RCP4.5), for the Thames-Coromandel district, given the higher values evident for this area relative to other parts of the Waikato region. Extreme precipitation is projected to increase by 5.43% for a 20-year ARI, by 5.94% for a 50-year ARI, and by 6.30% for a 100-year ARI (Median).

Table 6 Extreme daily precipitation change (mm/day) for the Thames-Coromandel District: Baseline and 2070 (RCP4.5) change (percent change). Results from the 22-GCM ensemble: Low, Median and High percentiles.

ARI (year)	Baseline (mm/day)	Low %	Median %	High %
5	161.46	2.53	3.94	5.17
10	191.13	2.34	4.81	5.37
15	208.82	2.68	5.15	6.39
20	221.65	2.72	**5.43**	6.46
30	240.24	2.80	5.68	7.65
40	253.82	2.87	5.81	7.77
50	264.62	2.94	**5.94**	7.88
100	299.72	3.27	**6.30**	8.52
150	321.48	3.60	6.40	9.26
200	337.52	3.85	6.47	9.86
300	361.02	4.21	6.60	10.77

Extreme daily precipitation is projected to increase from 234mm/day (Baseline) to 254mm/day by 2070 (RCP4.5) and to 256mm/day by 2100 (RCP4.5) for a 20-year ARI for the Thames-Coromandel district. For a 100-year ARI, extreme precipitation increases from 297mm/day (Baseline) to 326mm/day by 2070 (RCP4.5) and to 328mm/day by 2100 (RCP4.5). Changes to the ARI values for a particular extreme daily precipitation intensity value (mm/day) can also be evaluated. For instance, an extreme daily precipitation value of 297mm/day with a 100-year ARI (Baseline) is projected to have an ARI of 75 years by 2030 (RCP4.5), and an ARI of 52 years by 2070 (RCP4.5) (where the hashed line intersects with the RCP4.5 2030 and RCP 4.5 2070 trend lines, respectively).

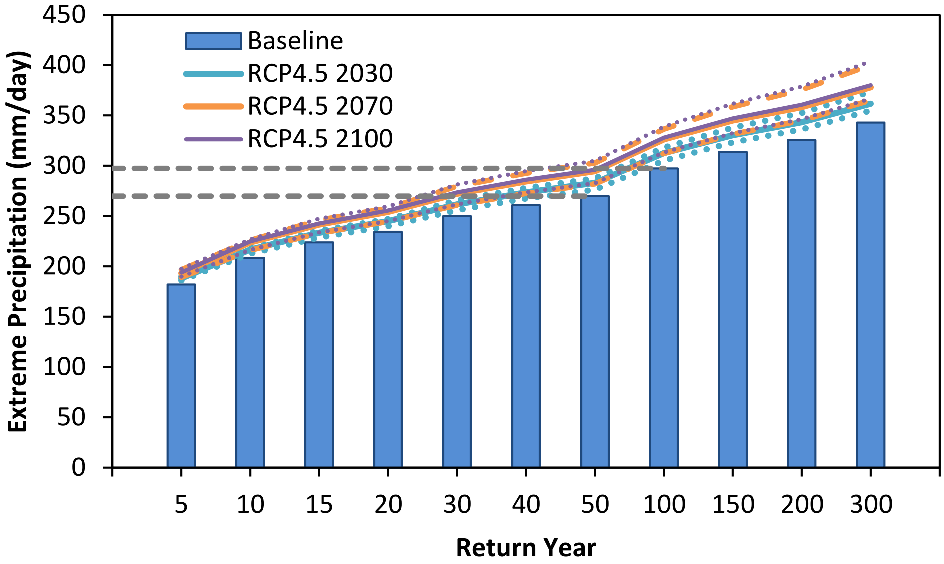

Figure 12 Changes in extreme daily precipitation (mm/day), for the Thames-Coromandel area. The blue bars indicate the baseline extreme precipitation values, and the coloured solid lines show the future projections of extreme precipitation per ARI using RCP4.5: 2030 (blue), 2070 (orange) and 2100 (purple) with corresponding coloured dashed lines representing the respective 25 and 75 percent confidence intervals.

2.2.4 Discussion and conclusion

The analyses found that all 22 GCMs project an increasing trend in extreme daily precipitation for the Waikato region for 2030, 2070 and 2100 scenarios. This is a noticeable difference with mean annual precipitation change (where both decreases and increases were evident). This pattern is consistent with climatological theory (Emori and Brown, 2005; Cubasch et al., 2001; Trenberth, 1999). In this report the direct results from GCM extreme daily precipitation scenarios for the Waikato region were used. As a result, our values are a little lower than global mean in extreme daily precipitation percent change, which is approximately 6% per degree global warming for 20 year return event using the AR5 data (Kharin et al, 2013).

The median changes in extreme daily precipitation for the Waikato region are spatially variable, increasing between 7.1-10.4% (RCP4.5) and 11.9-17.5% (RCP8.5) by 2070 and between 7.4-11.4% (RCP4.5) and 18.2-28.1% (RCP8.5) by 2100, as shown in Figure 11. Changes by 2030 were less than this, with a median change between 3.7-5.8% under RCP4.5 and 4.4-6.6% under RCP8.5. Therefore, by 2070 and 2100 the changes projected are higher than the global mean of 6% projected per degree global warming. This spatial variability in extreme daily precipitation change is characteristic of broader New Zealand trends reported (MfE, 2008).

Note: MfE (2008) suggest that even a 30-year run for a particular model is probably not long enough to get stable statistics of extreme precipitation events. **Therefore MfE recommends, that the same changes to rainfall return periods be applied everywhere across New Zealand.** The recommended adjustment factors are given in Table 5.2 of the MfE report, with an example in Appendix 4 (MfE, 2008). This recommendation should be taken into consideration, in assessing the above results.

2.3 Peak streamflow change

2.3.1 Introduction

Various studies report that as a result of climate change, heavier and/or more frequent extreme rainfall events are expected over New Zealand, especially in areas where the mean rainfall is projected to increase (MfE, 2010; IPCC, 2013). The inter-annual variability in rainfall in particular, as well as extreme rainfalls that induce floods, are influenced by the ENSO (El Niño Southern Oscillation) patterns in the South Pacific region. The ENSO effect is expected to maintain its influence on regional climate, with extreme high rainfalls projected coincident with La Niña phases of the ENSO, and extreme low rainfall events coincident with El Niño phases of the ENSO (IPCC, 2007b). The percentage increase in extreme rainfall intensity is expected to be approximately 6% per degree global warming (Kharin et al, 2013). In this report, extreme stream flow at each ARI value was calculated using the General Extreme Value (GEV) distribution and the *L*-moments parameter estimation (Walpita-Gamage et al., 2009; Malamud and Turcotte, 2006).

2.3.2 Methodology and data

As described in MfE (2010), increases in extreme rainfall are expected to represent the major impact of climate change on New Zealand river floods, while in coastal river reaches, sea-level rise will also affect inundation. Due to the complexity of the hydrological relationship between rainfall intensity and peak flow, and the uncertainty of projections of precipitation change, this report uses a method that is most commonly in use and provides a simple Rational Method (MfE, 2010). The equation for the Rational Method is provided below (as per MfE, 2010) as:

$Q = C\, i\, A\, /3.6$

Where,

Q is an estimate of the peak design discharge in cubic meters per second (m^3/sec)

C is the run-off coefficient

i is the rainfall intensity in millimetres per hour for a duration equal to the time of concentration of the catchment, and

A is the catchment area in square kilometres

However, as MfE (2010) points out, the relationship between rainfall intensity and flood magnitude depends on several factors that do not have a linear relationship; such that, for example, an 8% increase in rainfall intensity may not result in an 8% increase in flood peak discharge, or subsequently an 8% increase in flood inundation. Therefore, understanding of rainfall–runoff inundation processes also needs to be integrated in hydrological modelling efforts as these relate to an increase in rainfall.

The Rational Method is an empirical method to estimate peak flow. It is characterised by several features: rapid implementation, low data requirements, widely used in the engineering community, guidelines for estimating run-off coefficient are available. However, it is not suitable where rainfall varies significantly across the catchment, and it does show limited accuracy in validation tests. The Rational Method only needs rainfall intensity and run-off coefficients, which depend on catchment characteristics (i.e., slope, land cover, soil), the time of concentration and catchment area (MfE, 2010).

The future extreme peak flows were calculated using the flood estimate recommendations from MfE (2010). Changes to peak flows were projected using climate change scenarios for 2020, 2050 and 2100. The stations were chosen on the basis of having complete records for 30 or more years, as is standard methodology in climate change impact assessment (Martin and Parry, 1999). Two streamflow stations were selected to analyse historical streamflows in the Waikato region: (1) Kauaeranga station, on the Kauaeranga River, and (2) Te Aroha station, on the Waihou River. Both stations are located in the north-eastern part of the region in the Thames-Coromandel and Hauraki Districts, respectively (see Figure 13).

Figure 13 Map of the two stream flow stations used for the analysis of changes to extreme stream flow (Source: EW GIS layers).

2.3.3 Results

2.3.3.1 Baseline and future peak streamflows

The Thames-Coromandel and Hauraki Plains (where the two rivers traverse) are identified by Waikato Regional Council as 'Risk Areas' prone to large flood events. The Thames-Coromandel has very steep and small catchments with short run-off distances to rivers and is an area that is susceptible to tropical storm activity, while the Hauraki Plains have low-lying farmland and towns along the Waihou and Piako river systems that are vulnerable to flooding (see http://www.ew.govt.nz/environmental-information/Regional-hazards-and-emergency-management/River-flooding/#Heading1).

For the Waihou River, using an ARI of 100 years, Figure 14 (top figure) shows that the peak flow volumes are projected to increase from ca 578m^3/sec to ca 636m^3/sec by 2070 (RCP4.5) and to ca 640m^3/sec by 2100 (RCP4.5). An ARI of 50 years is projected to increase from ca 480m^3/sec to ca 524m^3/sec by 2070 (RCP4.5) and to ca 526m^3/sec by 2100 (RCP4.5). For the Kauaeranga River, for an ARI of 100 years, Figure 14 (bottom figure) shows that the peak flow volumes (m^3/sec) are projected to increase from ca 1135m^3/sec to ca 1249m^3/sec by 2070 (RCP4.5) and to ca 1256m^3/sec by 2100 (RCP4.5). An ARI of 50 years is projected to have increases in peak flow volumes from ca 1038m^3/sec to ca 1134m^3/sec by 2070 (RCP4.5) and to ca 1140m^3/sec by 2100 (RCP4.5). Compared to the previous results, the new projected peak flow is lower, since the increase in extreme precipitation using AR5 data is smaller.

The parallel dashed lines in Figure 14 show the change in ARIs over time. For example, an event with an ARI of 100 years in the baseline period is ca 578m^3/sec in Te Aroha. This peak flow value of 578m^3/sec, intersects the RCP4.5 2100 curve at an ARI of ca 78 years. This therefore projects that an event that has a current ARI of 100 years becomes an event with a projected ARI of 78 years by 2100 (RCP4.5). Corresponding changes to other ARI values are also illustrated in Figure 14.

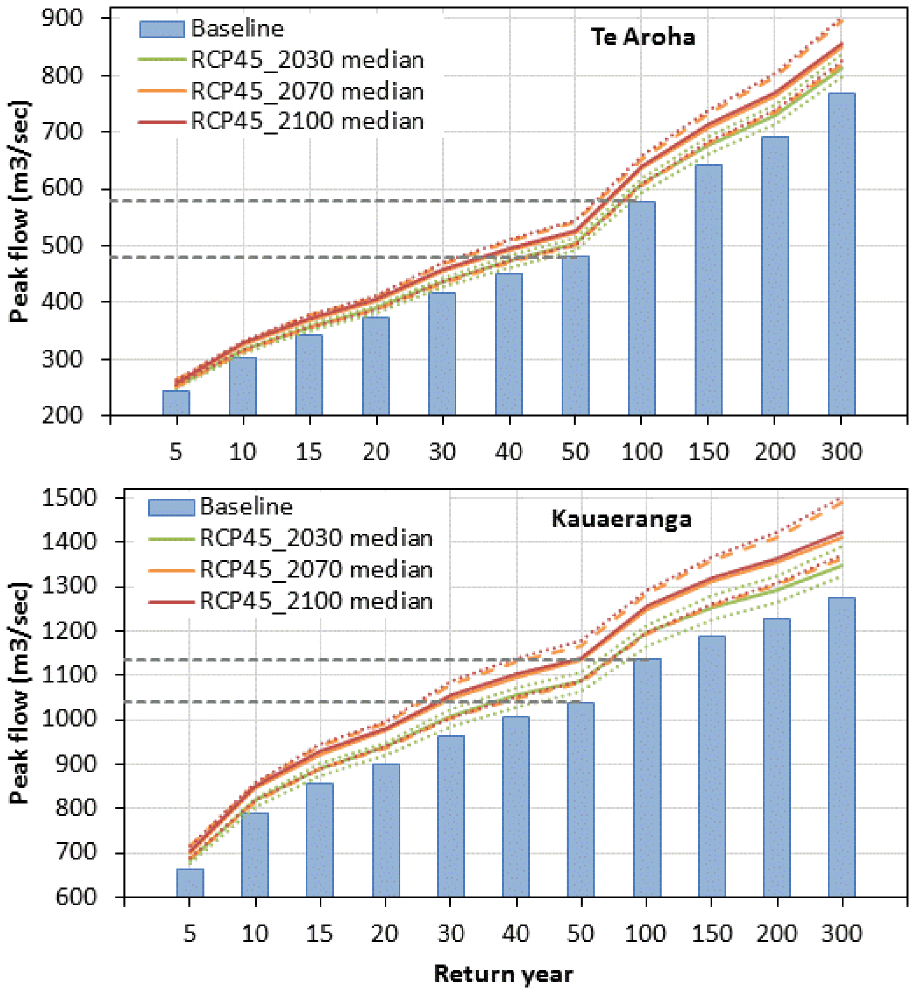

Figure 14 Peak flows (m^3/sec) and corresponding ARI values for baseline and future climate change scenarios for the Waihou River, (station at Te Aroha) (top figure) and the Kauaeranga River (station at Kauaeranga station) (bottom figure) for 2030, 2070 and 2100 using RCP4.5.

2.3.4 Discussion and conclusion

Climate change is projected to increase projected extreme peak flow in rivers such as the Kauaeranaga River and the Waihou River of the Waikato region. Additionally, climate change is projected to decrease the ARIs for peak flows relative to the baseline period. This is consistent with the projections at the national level for New Zealand in studies such as those of MfE (2010).

Other streams and rivers in the Waikato region also can be assessed for the impact of climate change on peak flows, however, the ones that have been selected here are for areas that are already known to be in hotspots of flood risk and therefore provide a relevant indicator of potential changes for the future.

2.4 Potential Evapotranspiration Deficit (PED)

2.4.1 Introduction

The majority of climate change scenarios, project decreases in precipitation for the eastern regions of New Zealand in the future, resulting in the eastern parts of the country experiencing more frequent drought events by the end of the 21st century, if greenhouse gas emissions continue to rise (Mullan et al., 2005). This has implications then, for the eastern parts of the Waikato region over the coming decades, and needs to be assessed for the extent and severity of the likely impacts. Drought occurrences affect agriculture and water resource management in particular, and the long-term planning for these sectors (Mullan et al., 2005; Jones, 2001).

2.4.2 Methodology and data

In order to compare the results produced in this Assessment with those of the national drought assessment (Mullan et al. 2005), the Potential Evapotranspiration Deficit (PED) was calculated for the baseline period (1976-2008), using the methodology in Mullan et al., 2005. Further details of the PED calculation are provided in Appendix 4.

Translating PED index values into drought severity thresholds that are applicable across the country is complicated, since a similar PED level in one region for which it is noted that farmers can adapt to, may cause adverse effects in other parts of the country that are accustomed to wetter conditions. For instance, in the drier eastern regions a PED of 200mm results in ca 1.5-2 months of water deficit, and 600mm to ca 5 months. For pasture-based agricultural systems, this would mean that when PED>200mm, there are up to 2 months of the year when there is insufficient water available for pasture growth (assuming that there is no irrigation to ameliorate the effects of the water deficit).

A worst case scenario, when PED>200mm and PED>400mm, was calculated using the future scenarios for a combination of the High (25^{th} percentile of the ensemble) of global temperature change and a Low (75^{th} percentile of the ensemble) of global precipitation change (using RCP4.5). The rationale for this combination is to test, future climatic conditions with a high temperature increase and low precipitation increase that result in intense dry climatic conditions. The worst case combination is presented to reflect the full range of possible changes to PED, although this situation is less likely to occur.

2.4.3 Results

2.4.3.1 Baseline and future Potential Evapotranspiration Deficits

Figure 15 shows the percentage of years, over a 30 year virtual period, with values for PED>200mm. For 2030, 2070 and 2100 scenarios, the 30-year virtual period is taken as 2016-2045, 2056-2085 and 2086-2115, respectively.

The results indicate a 'hotspot' of PED in the north-eastern parts of the Waikato region, mainly on the border between the Hauraki and Thames-Coromandel districts and south into parts of the Matamata-Piako and Waikato districts in baseline. However, because of the favourable change in precipitation in AR5, the PED in this area changes scarcely in the future. This is the noticeable difference between two results calculated from AR4 and AR5 data.

Additionally, in parts of the South Waikato, Rotorua and Taupo districts, PED increases a little by 2100. By 2070, between 49.5-74.1% of years in a 30-year period, centred around 2070, have a PED>200mm in the Hauraki district and parts of Thames-Coromandel district.

Table 7 provides percentage values of the whole Waikato for comparison.

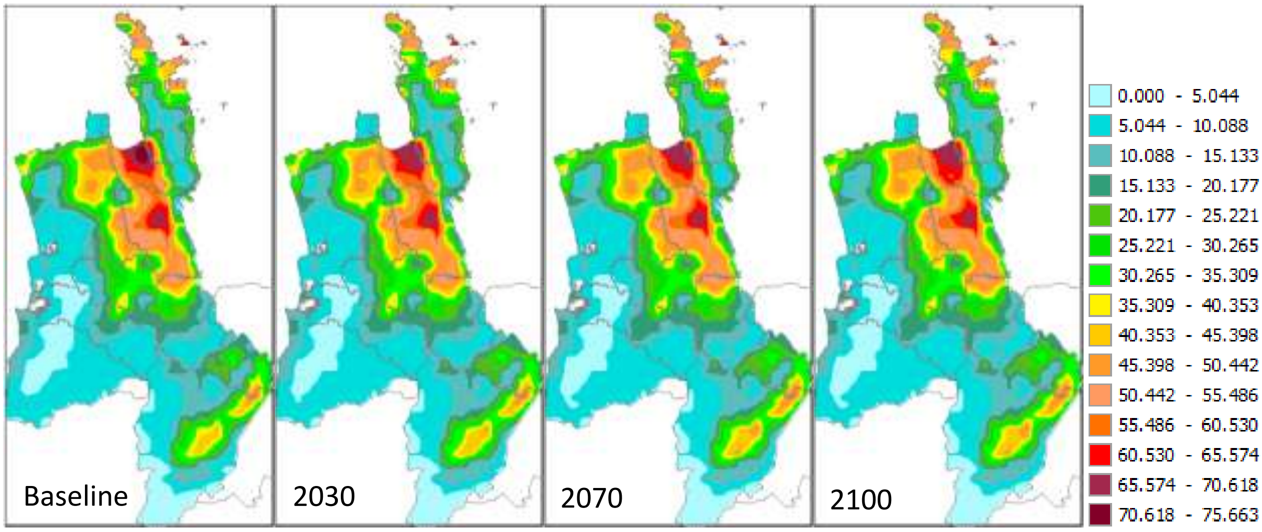

Figure 15 Percentage of annual PED by 2030, 2070 and 2100, where PED>200mm (RCP4.5, median)

Table 7 Percentage of PED>200mm and PED>400mm during the baseline and under the RCP4.5 scenario.

		Low	Median	High
PED >200mm	**Baseline**	15.03		
	RCP4.5 2030	10.21	15.05	19.41
	RCP4.5 2070	6.69	15.09	23.85
	RCP4.5 2100	6.30	15.09	24.51
PED > 400mm	**Baseline**	0.21		
	RCP4.5 2030	0.07	0.22	0.43
	RCP4.5 2070	0.01	0.21	0.86
	RCP4.5 2100	0.01	0.21	0.91

Figure 16 presents the worst case scenarios (RCP8.5) where PED>200mm and PED>400mm. For the baseline period, the occurrence of areas where PED>400mm is minimal (Figure 16xx, bottom panel). However, by 2070 and 2100 areas where PED>200mm and PED>400mm are projected to increase in spatial extent (Figure 16xx top and bottom panels). Extensive parts of the Hauraki and Matamata-Piako districts experience up to 71-97% of years when PED>200mm, over a 30-year period centred around 2100. Thames-Coromandel, Matamata-Piako, Waipa, Taupo and Rotorua districts also experience 71-97% of a 30-year period, centred around 2100, when PED>400mm. However, the effect is more restricted spatially than when PED>200mm.

Figure 17xx shows the percentage change in PED>200mm and PED>400mm by 2030, 2070 and 2100. The occurrence of PED>200mm is projected to ca 15.1 % by 2070 (RCP4.5 and RCP8.5) and ca 15.4% by 2100 (RCP8.5), while the percentage change in occurrence of PED>400mm increase minimally to ca 0.22% by 2070 (RCP4.5 and RCP8.5) and ca 0.25% by 2100 (RCP8.5). The box plots also indicate that the uncertainty associated with PED in 2100 is quite high.

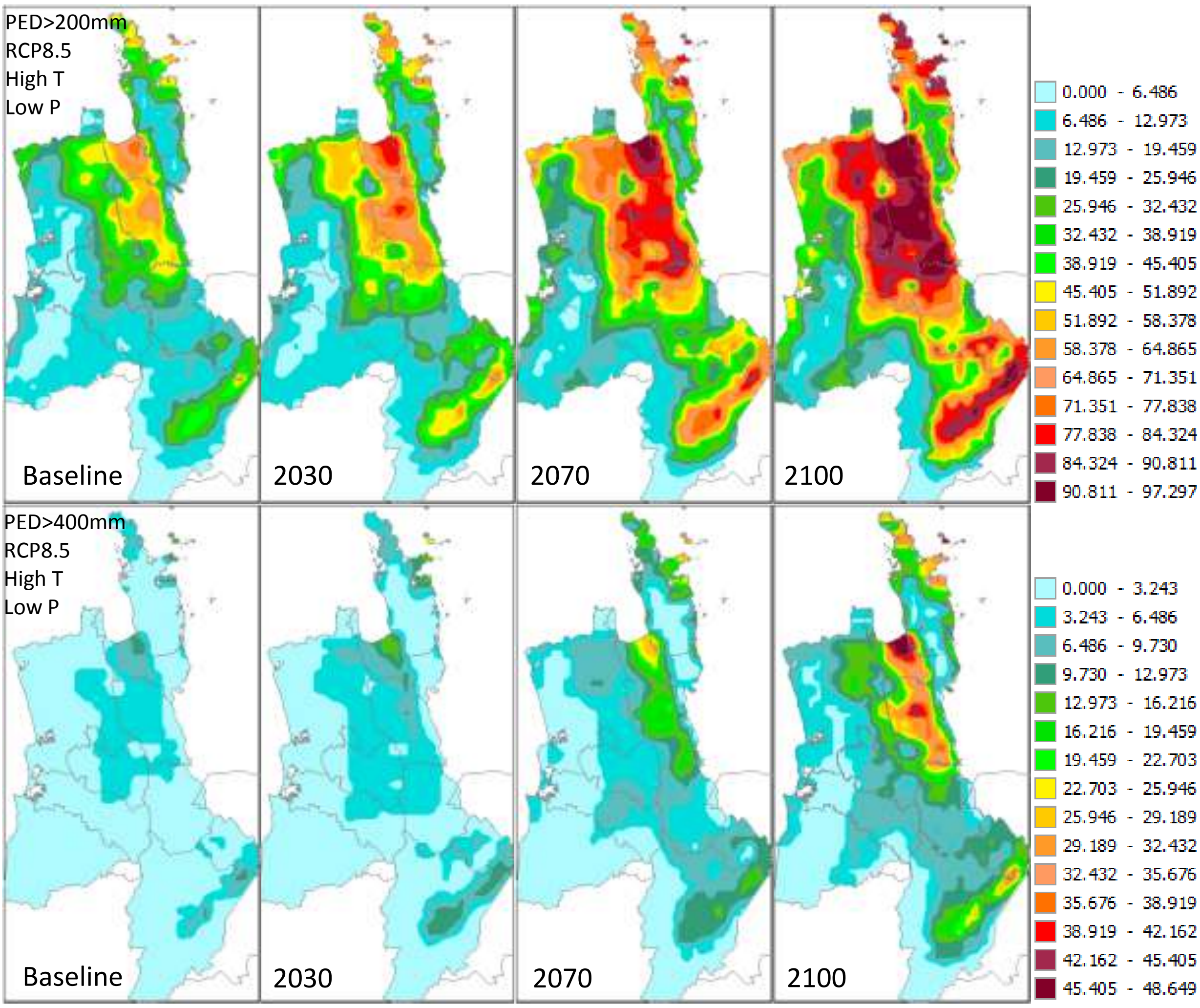

Figure 16 The worst case scenario for PED, combining a High (75th percentile) of GCMs for temperature change and Low (25th percentile) of GCMs for precipitation change under RCP8.5 scenario.

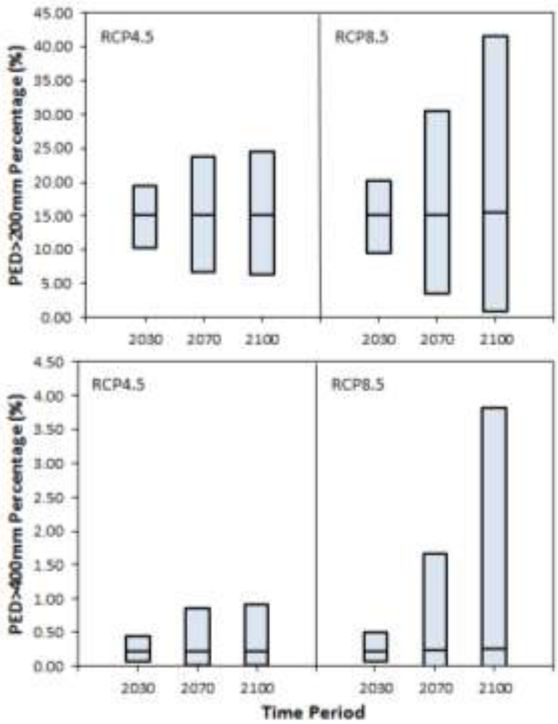

Figure 17 Percentage change in PED>200mm and PED>400mm: RCP4.5 and RCP8.5 for 2030, 2070 and 2100 for Waikato.

Figure 18 (top panel) shows the annual variation of PED for the baseline period for the Hauraki district. The July 2007–June 2008 period was the driest year in the time series, when the average PED was as high as 356mm (Median). The 2007/2008 summer-autumn was considered to represent a widespread drought event for most parts of the country, with the Waikato region incurring the highest dairy-related drought costs of $779 million (Butcher Partners Ltd, 2009). The lowest PED values for this time series were in 1983-1984, with a PED of 38.3mm (Median). The green bars indicate that the PED shows spatial variability across the Hauraki district, even though it is not a large district.

Figure 18 (bottom panel) illustrates changes in PED that have been perturbed to provide future change values by 2070 and 2100. The perturbation is also called a ‘change factor’, and involves adding the change factors of monthly mean changes for future scenarios to the historic observed daily data to form a new time series that represent the future climate conditions. For example, mean temperature in January is projected to increase by 1.2^{o}C by 2070 (RCP4.5). Thus this 1.2^{o}C change factor is added to each day in January for every year in the time series. This time series becomes the representative time series centred around 2070 (A1B). By using this perturbed future time series, the future PED is calculated (Figure 18xx (bottom panel)). Thirteen out of 32 years in the baseline period had values for PED>200mm, this is projected to increase to 12 out of 32 years by 2100. This projection is 5 years less than the previous result using AR4 data.

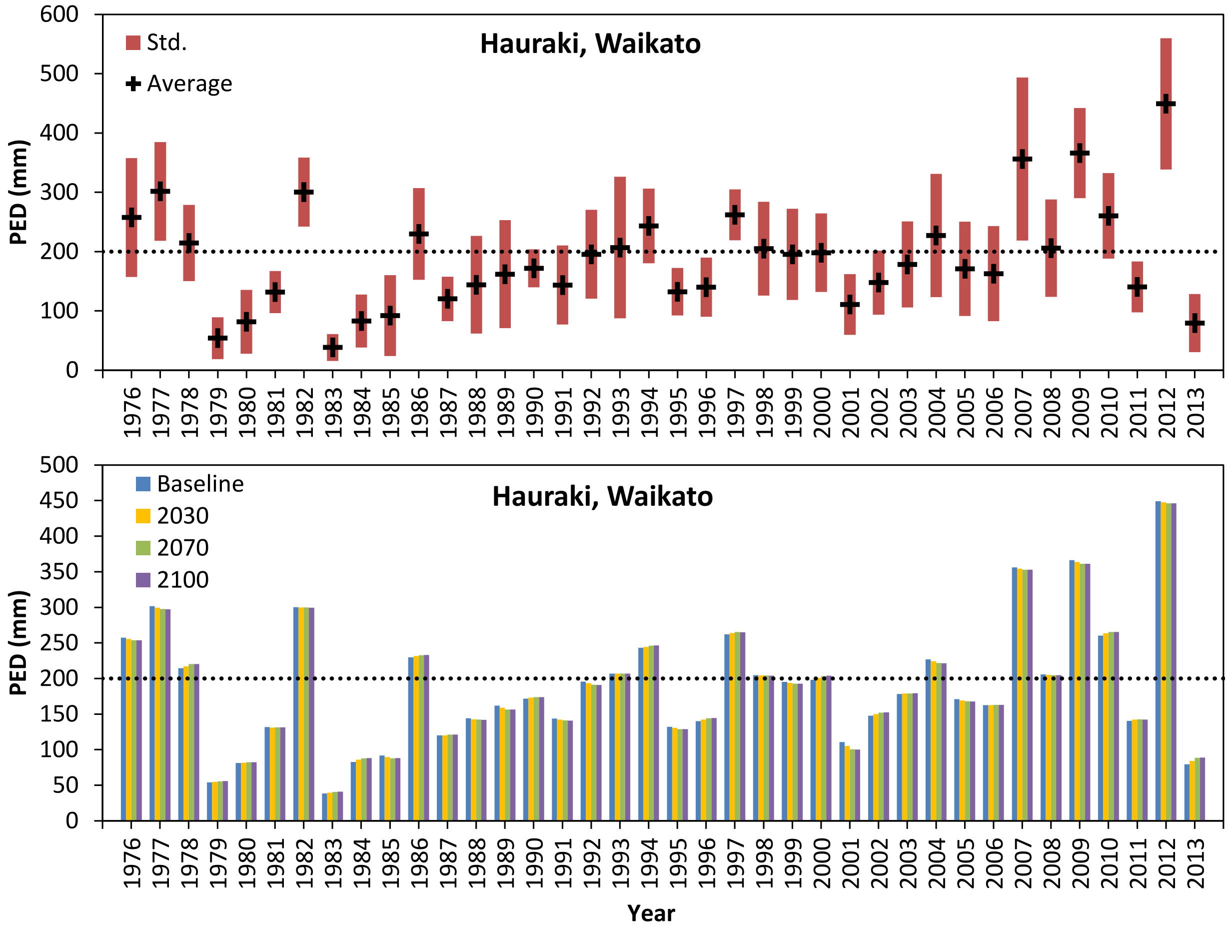

Figure 18 Annual variations in baseline PED (mm) (top panel) and the changes to PED (mm) with climate change (RCP4.5 for 2070 and 2100) (bottom panel) for the Hauraki district. The bars show the variations among years for the 49 PED spatial grid cells that cover the Hauraki district.

2.4.4 Discussion and conclusion

PED is a useful index of the change in drought potential in the Waikato region under baseline and future scenarios. The spatial patterns produced in Figures 15xx and 16xx indicate that the projected hotspot of future drought exposure is in parts of the Hauraki district (up to 44% of years in a 30-year period centred around 2100 when PED>400mm), followed by the Matamata-Piako and Thames-Coromandel districts, (where localised areas have up to ca 35% of years in a 30-year period, centred around 2100, when PED>400mm) particularly by 2100.

Although the median projection of PED does not change too much in the future, under a high temperature increase and low precipitation increase scenario, the Waikato is projected to have significant areas that are exposed to PED>200mm from 2070 onwards that could eventuate in increased drought risk and reduced water availability for pasture growth (up to 2 months per year likely). This intensifies by 2100 for parts of the Hauraki, Matamata-Piako and Coromandel districts (for PED>400mm that may result in 3-4 months of water deficit for pasture growth).

The spatial scenarios of PED change patterns are valuable in identifying areas with higher drought potential for regional planning purposes. However, PED values must be interpreted with regard to other factors that increase or reduce drought vulnerability of human and ecological systems. Additionally, Mullan et al. (2005) suggest that it is easier to define an index such as the PED from a science perspective, than it is to ensure that this index is the most suitable one for the intended purpose. Hence they suggest that the limitations of a proposed index should be clear, and left open for ways in which it might be improved.

Mullan et al. (2005) notes that an index is needed that is appropriate for both national and regional analyses and that it should adequately cope with differing thresholds and scales of drought severity. It should also be suited for estimating drought risk for agricultural landscapes in New Zealand with associated agricultural production losses linked to both the duration and intensity of drought events. The descriptor of drought may need to include climatological and hydrological information, as well as information on crop and animal production performance and a soil moisture deficit related index, depending on whether one is describing meteorological drought, hydrologic drought or agronomic/agricultural drought (MAF, 2009)[3].

2.5 Temperature-Humidity Index (THI)

2.5.1 Introduction

The Temperature-Humidity Index (THI) is a measure that combines effects of high ambient temperatures and relative humidity. It is a useful index to assess the risk of heat stress to

[3] 1) Meteorological drought: the state of the climate system that creates abnormally dry weather, prolonged enough for the lack of rainfall to cause serious hydrological imbalances; 2) Hydrologic drought: A deficit of water in the landscape, either in ground water reserves or in the surface hydrological system such as rivers, streams, and lakes; and 3) Agronomic/agricultural drought: A protracted period of deficient precipitation resulting in extensive damage to crop/pasture growth and production (MAF, 2009).

animals such as dairy and beef cattle in particular (Hahn et al., 2009; Bouraoui et al., 2002), though it is also applicable to human physiology and to other species. Studies have shown that dairy milk production and breeding efficiency of cows decrease with increasing thermal heat stress, for example, in Mediterranean climates (Bouraoui et al., 2002; Ingraham et al., 1975) and at extreme levels can endanger livestock (Hahn et al., 2009). However, other studies such as that of Dragovich (1979) highlight the fact that THI values need to be assessed in combination with other limiting factors. In general though, the THI index does capture much of the impact of warm to hot thermal environments on animals, by combining temperature and humidity parameters (Hahn, 2009).

2.5.2 Methodology and data

Details of the calculation of the THI used in this Assessment are shown in Appendix 6. The threshold values for THI are similar to those used by Dairy Australia, (under the programme 'Cool Cows: Dealing with heat stress in Australian dairy herds'. See also: de la Casa and Ravelo, 2003). The thresholds used for the THI are as follows:

1. If THI>72 (mild stress), cows are likely to begin experiencing heat stress and the in-calf rates will be affected;
2. If THI>78 (moderate stress), cows' milk production is seriously affected;
3. If THI>88 (severe stress), very significant losses in milk production are likely, cows show signs of severe stress and many ultimately die.

THI does not account for solar radiation or air movement (wind speed). However, both of these factors along with air temperature and relative humidity will influence the heat exchange of the animals with their surroundings (Bouraoui et al., 2002).

2.5.3 Results

2.5.3.1 Baseline and Future Temperature Humidity Indices

The number of days with THI>72 (mild stress) and the number of days with THI>78, (moderate stress), for baseline and future 2030, 2070 and 2100 scenarios (using RCP4.5) are shown in Figure 19xx. For the baseline period, the central parts of the Waikato region including Hauraki, Matamata-Piako, Waikato, Waipa and Otorohanga districts experience more days when THI>72, than the rest of the region. The highest number of days appears in the Hauraki district and parts of Matamata-Piako district, with between 54-66 days. However, by 2070, all the central areas of the Waikato region will have greater than 72 days when THI>72, and greater than 84 days when THI>72 in the Hauraki district and in parts of Matamata-Piako district. By 2100, large parts of the Waikato region experience 72>THI, with the largest number of days being located in the Hauraki, Matamata-Piako, Otorohanga, Waipa, Waikato and Thames-Coromandel districts.

With respect to the number of days when THI>78, Figure 19 (bottom panel) shows that this is negligible during the baseline period, such that there are no locations where the average number of days when THI>78 is more than 1 day. However, by 2070 (RCP4.5), Matamata-Piako and Otorohanga districts are projected to have up to 6 days when THI>78. Most parts of the central Waikato are projected to have between 4-6 days when THI>78 by 2100.

The average number of days when THI>72 is projected to increase to ca 56 days (RCP4.5), 70 days and (RCP8.5) by 2070, and up to 88 days (RCP8.5) by 2100 (Figure 20, top panel). The average number of days when THI>78 is projected to be minimal for 2030 and 2070 scenarios and increases by up to 2 days by 2100 (RCP4.5) and by up to 9 days by 2100 (RCP8.5) (Figure 20, bottom panel). The green bars for 2100 scenarios for both THI>72 and THI>78 indicate, however, that there is a wide spread of projections by the individual GCMs, particularly under RCP8.5, which is a measure of the uncertainty associated with projections of THI by this time period.

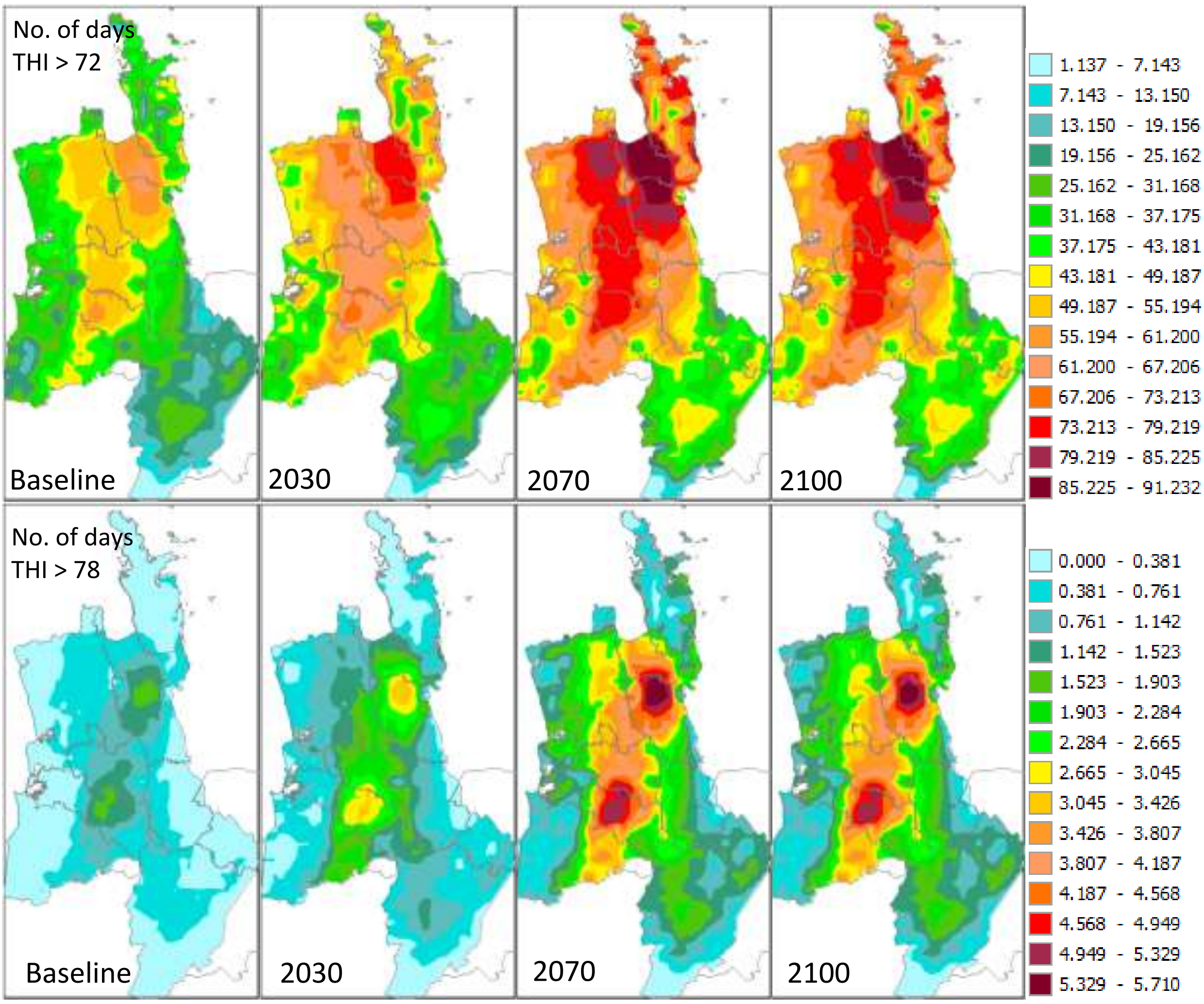

Figure 19 Number of days where conditions likely to induce mild stress (72<THI<78) (top panel) and moderate stress (79<THI<88) (bottom panel) to cattle, for baseline and future projections: RCP4.5 for 2030, 2070 and 2100 scenarios.

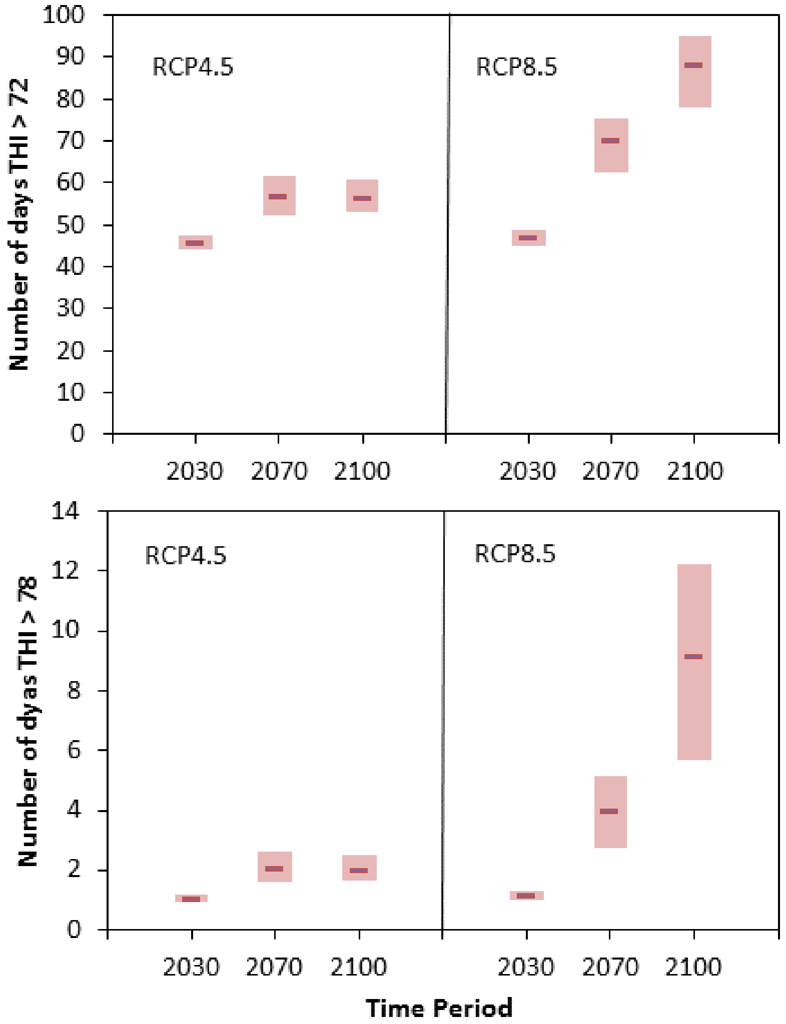

Figure 20 Change in average number of days per year when THI>72 (top panel) and THI>78 (bottom panel): RCP4.5 and RCP8.5 for 2030, 2070 and 2100 scenarios. Results from the 40-GCM ensemble, Low, Median and High percentiles represented by the red boxes and marks: the bottom and top of box are the low and high percentiles, and the mark in box shows the median projection of 40 GCMs.

Further analysis was done focusing on the Hauraki district, using historical temperature records (1976-2008) for this area, given that it is one of the hotspots for higher THI values in the future. Figure 21 (top figure) shows that on average, there were about 52 days per year when 72<THI<78 for the baseline period of 1976-2008, and this increases to an average of 66 days by 2030 (RCP4.5) and to an average of 63 days by 2010 (RCP4.5). Figure 21 (bottom panel), shows a wide variation among years, and that on average there was less than 1 day per year when 72<THI<78 was over the baseline period of 1972-2008. This increases to an average of 2 days by 2030 (RCP4.5) and falls back to an average of 1 day by 2070 (RCP4.5).

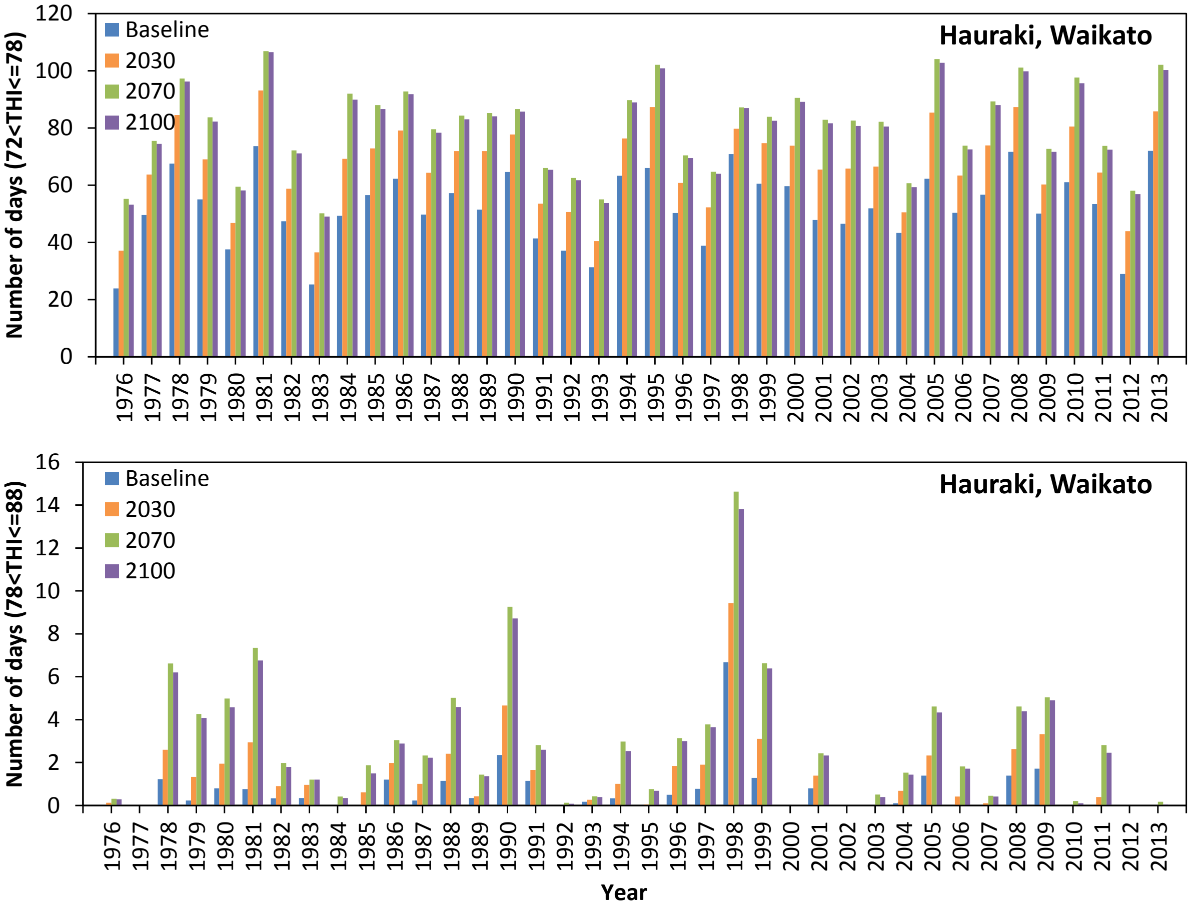

Figure 21 Variations in number of days when 72<THI<79 (top figure) and 79<THI<89 (bottom figure) in the Hauraki District: for Baseline, 2050 and 2100 (A1B) scenarios.

2.5.4 Discussion and conclusion

THI scenarios for the Waikato region provide a useful indication of the changes to thermal heat stress projected by 2030, 2070 and 2100. The spatial patterns in Figure 19xx illustrate that north-east and central parts of the Waikato region will be most affected by the intensifying THI values, particularly by 2070 and 2100. Similar to PED, the Hauraki and Matamata-Piako districts are a hotspot for increased THI values, along with parts of the Otorohanga district, and to a lesser degree parts of the Thames-Coromandel district. However, as Figure 20 shows, the scenarios for 2100 exhibit a wide range of modelled THI for individual GCMs in the ensemble (evident from the size of the green box by 2100), which is also a measure of the uncertainty associated with THI scenarios by that time horizon.

2.6 Growing Degree Days (GDD)

2.6.1 Introduction

Growing Degree Days (GDD) has been used as an effective measure of the amount of accumulated heat above a base temperature (at which growth processes are activated), to describe the length of the growing season and the timing of key lifecycle events for temperature-limited species (Kriticos et al., 2003; Ramankutty et al., 2002; Theurillat and Guisan, 2001; McMaster and Wilhelm, 1997). GDD can be used for both cultivated and wild species as well as species that pose a biosecurity risk to cultivation and biodiversity conservation. Conversely, GDD can also be used to identify areas where heat accumulation is insufficient, indicative of a cold stress influence on plant biological processes (Kriticos et al., 2003).

Various studies use GDD in combination with other climatic indices for applications such as: estimating field crop growing requirements (Basiden et al., 2008); estimating future species distribution changes with climate change (Kriticos et al., 2003); and changes in biosecurity disease risks (Sutherst, 1998) among others.

2.6.2 Methodology and data

There are various calculation methods in use for deriving GDD (Kriticos et al., 2003; Ramankutty et al., 2002; McMaster and Wilhelm, 1997). Here we use one of the more widely-used equations (McMaster and Wilhelm, 1997). To calculate GDDs for a site on a particular day, the daily mean temperature is calculated by averaging the maximum (highest) and minimum (lowest) temperatures for the day. Then a selected base temperature is subtracted from the mean temperature to get the number of GDDs for the 24-hour period. If the daily mean temperature is less than, or equal to the base temperature, the GDD value for that day is zero. This assumes that little or no growth takes place on those days.

The equation used to calculate GDD in this report is:

$$GDD= ((T_{max}-T_{min})/2)-T_{base}$$

2.6.3 Results

2.6.3.1 Baseline and future projections

GDD increases by ca 475.45˚D (RCP4.5, Median) or 711.01˚D (RCP8.5, Median) by 2070; and ca 473.90˚D (RCP4.5, Median) or 1076.89˚D (RCP8.5, Median) by 2100 for GDD>0˚C. The GDD values are much lower for GDD>10˚C (RCP4.5, Median), however the change relative to the baseline is ca 364.83˚D (RCP4.5, Median) or 587.0˚D (RCP8.5, Median) by 2070 and ca 360.5˚D (RCP4.5, Median) or 918.0˚D (RCP8.5, Median) by 2100. (These change values are calculated by subtracting the Baseline value from the future GDD projected value in Table 8). Figure 22 indicates the change in GDD above the three base temperatures, 0˚C, 4˚C and 10˚C.

Table 8 Regional average GDD for baseline and future scenarios: RCP4.5 and RCP8.5 for 2030, 2070 and 2100

		>0°C GDD			>4°C GDD			>10°C GDD		
Baseline		4763.91			3306.66			1342.14		
		Low	**Median**	**High**	**Low**	**Median**	**High**	**Low**	**Median**	**High**
RCP4.5	2030	4929.23	4965.26	5018.68	3501.98	3532.27	3570.06	1499.10	1527.02	1559.86
	2070	5134.57	5239.36	5334.80	3679.42	3767.27	3862.31	1637.76	1706.97	1793.03
	2100	5147.72	5237.81	5316.22	3689.46	3762.48	3847.21	1646.64	1702.65	1779.52
RCP8.5	2030	4946.57	5001.51	5050.99	3519.74	3556.55	3606.37	1514.72	1549.19	1582.35
	2070	5347.94	5474.92	5604.35	3878.34	3999.72	4112.16	1806.46	1929.14	2023.49
	2100	5654.82	5840.80	5971.35	4180.94	4408.95	4552.24	2062.45	2260.14	2397.46

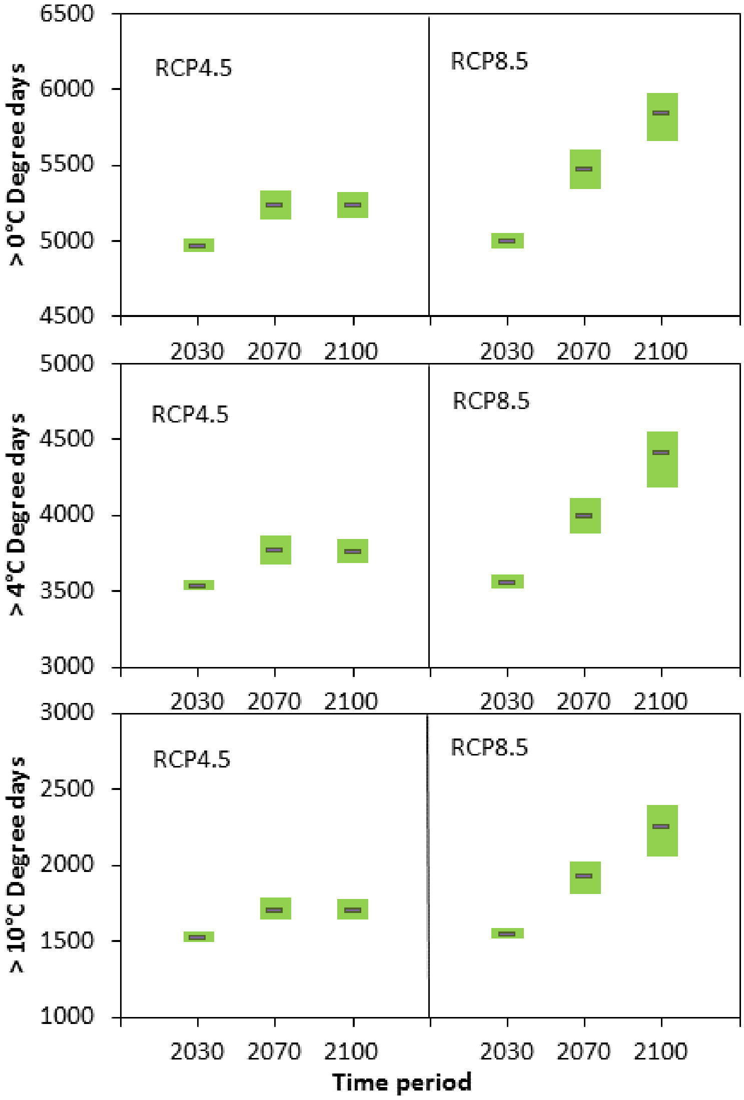

Figure 22 Change in average Growing Degree Days above three base temperatures 0°C, 4°C and 10°C for 2030, 2070 and 2100 (RCP4.5 and RCP8.5) scenarios. Results from the 40-GCM ensemble, low, median and high percentiles represented by the green boxes and marks: the bottom and top of box are the low and high percentiles, and the mark in box shows the median projection of 40 GCMs.

Figure 23 shows the baseline and future scenarios of the GDD using three alternative base temperatures: 0°C, 4°C and 10°C for 2030, 2070 and 2100 (RCP4.5). The GDD values increase in the northern districts of the Waikato region by 2030, 2070 and 2100, particularly in the Thames-Coromandel, Hauraki, Matamata-Piako, and Waikato districts. GDD increases the most above the base temperature of 0°C by 2070 and 2100.

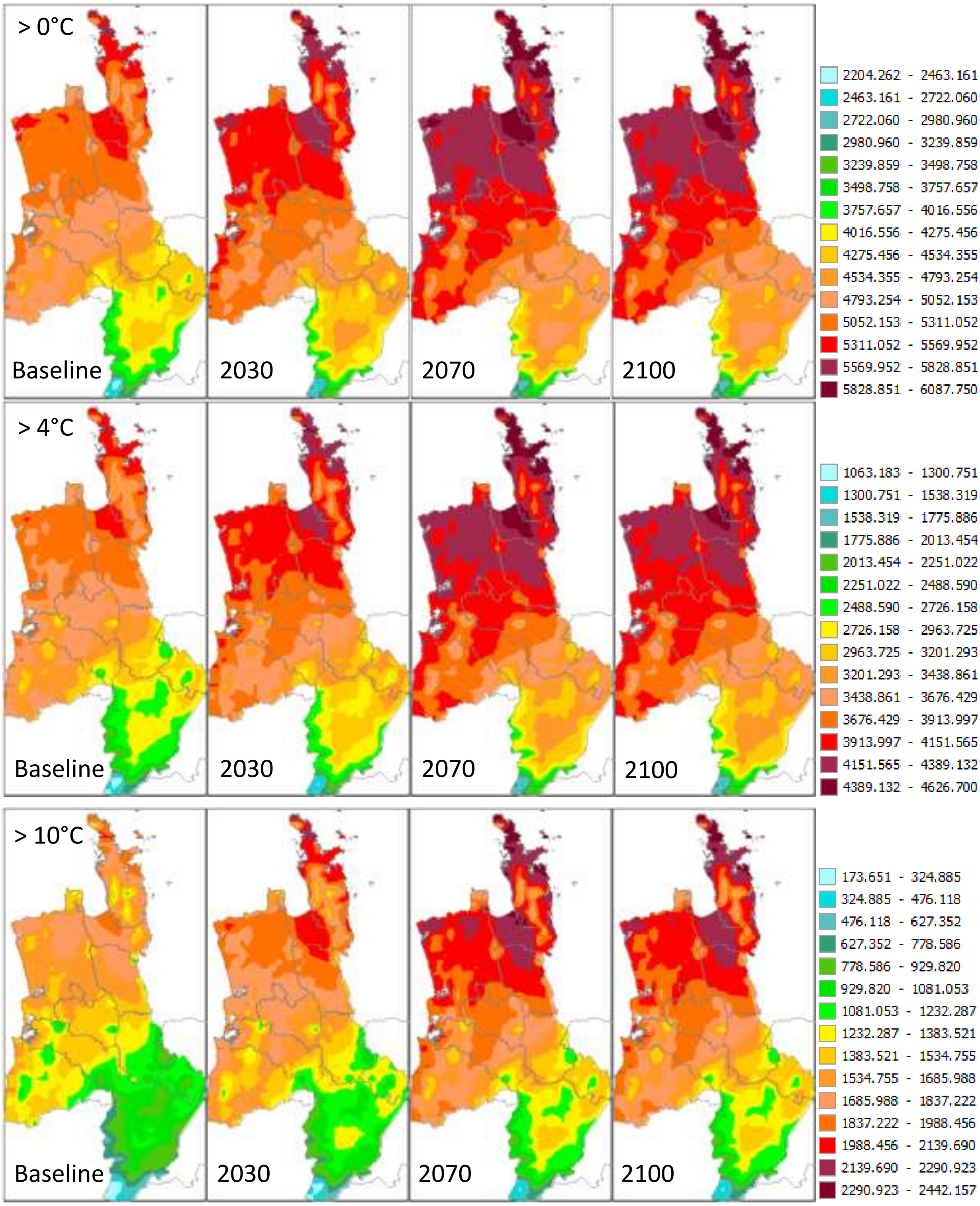

Figure 23 Growing Degree Days for base temperature >0°C, >4°C and >10°C: for baseline, 2030, 2070 and 2100 (RCP4.5) scenarios (unit: degrees).

2.6.4 Discussion and conclusion

The GDD future scenarios for 2030, 2070 and 2100 indicate that there will be a lengthening of the growing season for the Waikato region for species that require base temperatures such as 0°C, 4°C and 10°C to initiate growth. GDD increases by ca 473.9°D by 2070 and by 1076.89°D by 2100 for GDD>0°C (RCP4.5 and RCP8.5 respectively); and the increase is about 360.5°D (RCP4.5) by 2070 or 918.0°D (RCP8.5) by 2100 for GDD>10°C.

These results are consistent with the IPCC projection of changes to GDD for the North Island of New Zealand of between 500-800 degree days by 2080 (using a base temperature of 5°C) relative to the baseline period (IPCC, 2001). According to the MAF ECOCLIMATE report for New Zealand (Baisden et al., 2008), this increase in GDD may result in changes such as earlier start dates for pasture growth in late winter or spring. Overall, the changes indicated by GDD for the growing season provide a useful measure that indicates potential geographic shifts in agricultural productivity and seasonal growing patterns. These shifts must be interpreted in conjunction with other climate and production-related information for meaningful planning of adaptation options.

2.7 Extreme wind

2.7.1 Introduction

Wind extremes refer to extreme strong wind events over time. These extremes have attracted considerable research focus due to the potential hazards these present to human and natural systems. Extreme wind and storminess are projected to increase in winter but magnitude of change in the extreme wind speeds is not large at only a few percent by the end of this century under the middle-of-the range A1B SRES (Mullan et al. 2011). Only the baseline patterns of extreme wind are given in this report. However, with new methodologies and CMIP5 data becoming available (Chang et al. 2012), further study could be carried out. Methodology and data

The extremes of wind speed in the past are calculated using NIWA VCSN data (1997-2013) for 12 ARIs, i.e. 1, 5, 10, 15, 20, 30, 40, 50, 100, 150, 200, 300 year return. Peak of Threshold (POT) method was applied for extreme wind speed analysis, Generalised Pareto Distribution (GPD) distribution parameters were estimated using L-moments method (Hosking and Wallis, 1997).

2.7.2 Results

Figure 24 shows the historical **extreme wind speed** for an event with 1, 20, 50 and 100- year ARI. The hot spots of extreme wind event are Thames-Coromandel, Waitomo, Otorohanga, Rototura and Taupo Districts. The maximum extreme daily wind speed in Thames-Coromandel could be about 14m/s for normal years (i.e. 1-year ARI). The 100 year return extreme wind is 21.4m/s in Thames-Coromandel, 18.7m/s in Waitomo and Otorohanga, and in 18.3m/s Rotorua and Taupo, respectively.

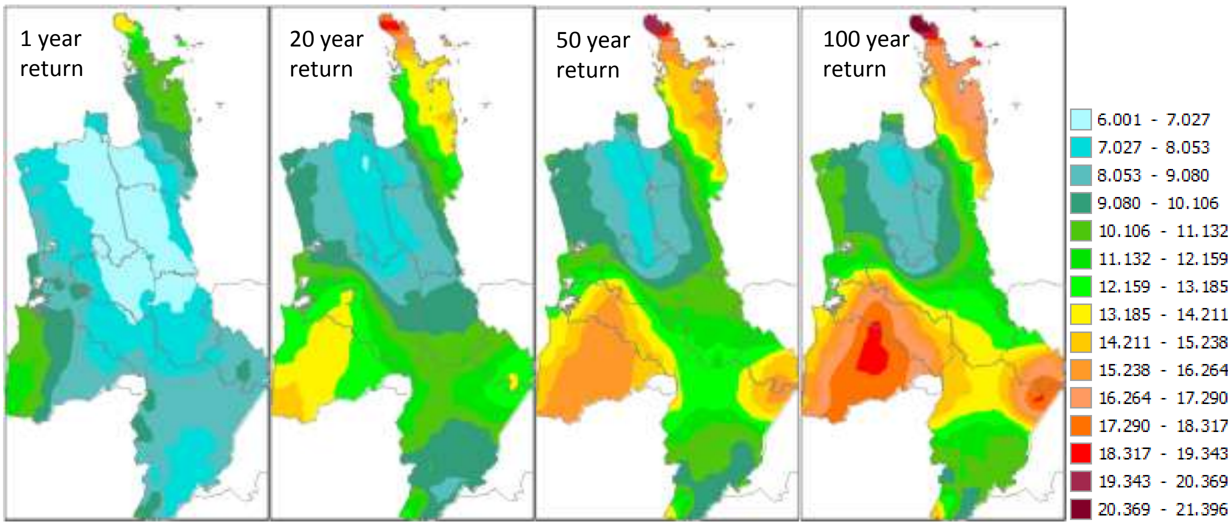

Figure 24 The historical extreme wind pattern of Waikato (1997-2013).

Table 9 The Extreme wind speed (m/s) for 12 ARIs in hot spot district

ARIs (year)	Thames-Coromendal	Waitomo	Otorohanga	Rotorua	Taupo
1	10.26	9.67	8.06	8.35	8.45
5	11.75	11.00	9.31	9.30	9.25
10	12.70	12.07	10.36	9.96	9.89
15	13.26	12.76	11.06	10.37	10.31
20	13.65	13.29	11.61	10.68	10.64
30	14.20	14.08	12.45	11.12	11.15
40	14.59	14.68	13.11	11.45	11.54
50	14.90	15.17	13.66	11.72	11.87
100	15.86	16.84	15.60	12.59	13.03
150	16.43	17.95	16.93	13.15	13.83
200	16.84	18.79	17.98	13.56	14.46
300	17.42	20.07	19.62	14.17	15.44

The daily wind speed may not reflect the extreme gust during a day, therefore the hourly wind speed at Whitianga (S36.834, E175.677) observation station which is a "Hot spot" in the Thames-Coromandel district, is further analysed (see Table 10). The maximum hourly wind speed for a 50 year return is about 17.77 m/s at Whitianga, and the value for 100 year return is about 18.41 m/s.

Table 10 The extreme hourly wind speed (m/s) for 12 ARIs at the Whitianga Site (1990-2005).

ARIs (year)	1	5	10	15	20	30	40	50	100	150	200	300
	13.84	15.52	16.22	16.62	16.90	17.29	17.56	**17.77**	18.41	18.78	19.04	19.40

3 Conclusions

This report provides an assessment of the key climate change impacts on the Waikato region in terms of projected changes by 2030, 2070 and 2100 using the IPCC AR5 data, for 9 climatic indices:

1. Mean temperature change
2. Mean precipitation change
3. Extreme precipitation change
4. Peak streamflow change
5. Potential Evapotranspiration Deficit (PED)
6. Temperature-Humidity Index (THI)

7. Growing Degree Days (GDD)
8. Extreme wind speed

Additionally, this report provides detailed spatial scenarios for all of the listed variables except peak streamflow change and sea level rise (when site specific projections are provided). The Assessment provides information that is relevant to medium- and long-term spatial planning for the regional and district councils.

The results provided indicate that mean annual temperature increases by 1.17°C by 2070 and by 1.25°C by 2100 (under the RCP4.5 scenario). Summer (DJF) and autumn (MAM) mean temperature increase is the highest seasonal change, 1.23°C by 2070 (RCP4.5) and by up to 1.27°C by 2100 (RCP4.5).

Mean annual precipitation change is highly variable, with both increases and decreases projected depending on the GCM used. This variability in the mean annual and seasonal precipitation projections (including the direction and magnitude of changes) indicates the inherent uncertainty associated with projections of precipitation change. The range of projected annual precipitation is between a decrease of 4.56% and in increase of 9.22% by 2070 (RCP4.5) and between a decrease of 4.84% and an increase of 9.9% by 2100 (RCP4.5). Seasonal mean precipitation changes include projections for winter (JJA) mean precipitation change of between -4.22% and 8.23% by 2070 (RCP4.5) and between -4.49 and 8.77% by 2100 (RCP4.5). Summer (DJF) mean precipitation is projected to change between -4.7 and 10.71% by 2070 (RCP4.5) and between -5.02 and 11.54% by 2100 (RCP4.5). The highest mean precipitation changes are projected for the Waitomo, Otorohanga, Thames-Coromendal and Taupo districts. The increase in autumn seasonal is higher than other seasons.

Extreme daily precipitation changes indicate an increase that is consistently located in north-east parts of the Waikato region – i.e. in the Hauraki and Thames-Coromandel districts and the northern part of the Waikato district.

Peak streamflow changes are expected to increase in rivers such as the Kauaeranga and Waihou rivers which were selected for further analysis on the basis that extreme precipitation increases were also projected to be highest in the areas through which these rivers flow. The Average Recurrence intervals (ARIs) for peak streamflows are also expected to decrease (i.e. peak streamflows of specific values occur more frequently), and are described further in this report.

Projections for changes to PED also highlight the spatial variability of impacts with the highest PED values (where PED>400mm) located in the Hauraki and Matamata-Piako districts by 2100 (RCP8.5 combining high temperature change and low precipitation change scenarios). However, PED>200mm (RCP4.5, combining high temperature and low precipitation scenarios) are more widespread across the Waikato region by 2070 and 2100, such that there will be an impact on most of the central, northern and eastern parts.

The THI index indicates that mildly stress-inducing conditions (THI>72) for animals such as dairy cows are widespread across the Waikato region by 2070 and 2100. Moderately stress-inducing conditions (THI>78) are more restricted to the central parts of the Waikato region by 2070 and 2100, with two ‘hotspots’ evident in the Hauraki and Matamata-Piako districts and further south in the Otorohanga district.

GDD projections indicate that a lengthening of the growing season is expected across the entire Waikato region, although the increase is spatially variable and highest in northern districts where temperatures are warmer and lowest in the Taupo district. This projected lengthening of the growing season is likely to have beneficial effects on pasture and crop productivity in itself, and may create opportunities for new commercial crops to be cultivated. This increase in GDD also may have an impact on native species or species of importance to biosecurity, where GDD changes are likely to induce more favourable growing conditions. However, the increase in GDD also should be assessed in conjunction with changes to other climatological indices that affect crop production and species distribution, given that areas that have the highest GDD increases also have the highest PED and THI values.

The hot spot of extreme wind event is in Thames-Coromandel, Waitomo, Otorohanga, Rotorua and Taupo district. The extreme wind speed is not projected to change much in the future.

The uncertainties associated with the future projections of the 8 climatic variables increase progressively between 2030 and 2100 scenarios, including uncertainties associated with future GHG concentration profiles, the earth's climate sensitivity to the GHG concentration, the extent of the effects of feedbacks mechanisms which may influence the rate and magnitude of climate change (IPCC, 2007a). The uncertainty has been represented in this Assessment by illustrating the spread of individual GCM projections within the various ensemble results.

Compared to the previous assessment, the increase of temperature is slightly lower and the decrease in annual precipitation is smaller as well when using AR5 data. The increase in extreme daily precipitation is only half of the previous results. So the increase in projected PED, THI and GDD are also slight smaller on average than their former values.

Particular attention needs to be given to the Hauraki and Thames-Coromandel districts, which are identified as hotspots of potential drought and flood-related impacts.

On the basis of these patterns, we provide the following recommendations for more in-depth impacts assessments that will inform adaptation options and processes for the Waikato region.

4 Recommendations and future research direction

Recommendation 1:

It is important for baseline and future climate change projections of the Waikato region to be integrated into Regional Council strategies including those for hazard management, biodiversity and biosecurity management, coastal area management, water and land management and regional planning. This will assist in mainstreaming climate change effects into Regional Council policy.

Recommendation 2:

The north-eastern areas represent a 'hotspot' of potential increased flood occurrence due to increases in extreme daily precipitation into the future. This warrants further localised and more detailed assessment using hydrological modelling approaches to assess flood risk with future climate change. For a comprehensive perspective of the vulnerability of communities and infrastructure to these risks, socio-economic and land-use related variables will need to be integrated in the scenarios.

Recommendation 3:

Drought-inducing conditions in the Waikato region, estimated using the Potential Evapotranspiration Deficit (PED) index, will increase into the future for a considerable part of the Waikato region, particularly in the Hauraki and Matamata-Piako districts. Given the dependence of the regional economy on agricultural pasture, crop and animal productivity, this warrants a more in-depth assessment of drought risk that climate change poses. In addition, drought risk needs to be integrated with other climatological and hydrological information, and information on agricultural productivity (as suggested by MAF, 2008). Hydrological drought also can impact urban water supply takes, sewerage treatment plant operations and irrigation takes and their impacts. Drought can also influence water quality such as algal blooms and lake water quality. The latter river and lake water issues are complicated and could be modelled in collaboration with others such as Professor David Hamilton and NIWA. Given the recent drought situations and climate change projections, further study on extreme drought event monitoring and forecasting needs to be carried out in relation to the aforementioned issues.

Recommendation 4:

Decreasing soil moisture availability, extent of streamflows and drought frequency and duration will have implications for water management. Thresholds for water scarcity for natural and managed systems will therefore need to be assessed and integrated in regional land-use scenarios to evaluate the level of risks into the future. The new soil moisture monitoring network data could be used in this modelling as well as WISE models which are already held by Waikato Regional Council and that could include updated climate modelling projections and potentially other modelling elements. Such landuse modelling and land management planning could be enhanced for such issues as effluent management through application of seasonal forecasting data and development of early warning or advisory systems for rural land managers.

Recommendation 5:

Moderate heat-stress conditions (dairy cows used as an example in this report) likely will increase into the future, particularly in the central districts, as indicated by the Temperature-Humidity Index (THI). It is therefore important to assess in greater detail the implications of thermal heat stress on animal welfare by integrating climate change and information on animal physiology. This would then form the basis for addressing adaptation options for reducing animal stress (e.g., shade protection, dietary modifications).

Recommendation 6:

The Hauraki, Thames-Coromandel, Matamata-Piako and the northern parts of Waikato districts are all identified as having the highest risk of exposure to extreme climatic events into the future in terms of precipitation. Therefore it is recommended that thresholds be determined for the likely implications of changing habitat conditions and ecosystem dynamics. A particular focus on the Significant Natural Areas (SNAs) located in the Hauraki district and surrounding areas is recommended.

Recommendation 7:

Historical extreme wind speed distribution was analysed in the report. Given the importance of storminess and extreme wind hazard impacts on infrastructure, especially on ports infrastructure, operations and planning, a further study on storminess and wave condition under climate change using emerging mythologies and CMIP5 data could to be carried out.

Extreme sea level events applying the latest CMIP5 data could also be considered for specific sites or coastlines such as the southern Huaraki Gulf and the peat lands to the south and the Thames area given the vulnerability identified in this region for extreme precipitation events which could coincide with extreme sea level events creating a potential mega extreme event.

Recommendation 8:

Biodiversity and invasive species concerns will be enhanced by climate change. There are a diverse range of risks in this area with invasive grass and weed species potentially threatening the rural economy while biosecurity concerns could shift with pests and diseases becoming a greater risk for establishment with higher temperatures and shifts in the precipitation regime. Further analysis of the risks for such events and the role of extreme events and slow onset climate change in the risk mix could be further examined.

Recommendation 9:

WEL Networks has signalled its growing interest in dispersed energy production from renewable sources such as wind and solar. The modelling of changes in the renewable mix in the region could be influenced by changes in climate and extremes for their on-going viability and efficiency. WEL Energy could be a possible partner in an examination of the risks in this area.

Related to power generation and disruption are the larger ‘lifelines’ risks for the region. The regions power transmission network, water supply infrastructure, critical roads, internet and medical facilities could be examined for the climate vulnerability. The increasing prevalence of severe storms (weather bombs) can be modelled and the potential risk to ‘lifelines infrastructure and services could be examined and disaster risk mitigation plans devised.

Recommendation 10:

One or more RAP (Rapid Assessment Program) workshops should be considered to bring together stakeholders on various issues noted in the recommendations. These workshops would aid in the resolving of issues regarding priorities in addressing a potentially large list of issues. RAP workshops could also be used to gather information of the range of potential partnering opportunities to deliver the required research and also identify funding opportunities to support it.

5 References

Alexander, L. V., & Arblaster, J. M. (2009). Assessing trends in observed and modelled climate extremes over Australia in relation to future projections. *International Journal of Climatology, 29*(3), 417-435. 10.1002/joc.1730

Baisden, T., Greenhalgh, S., Kerr, S., Newton, P., Renwick, J., Stroombergen, A., et al. (2008). *Costs and benefits of climate change and adaptation to climate change in New Zealand: what do we know so far?* : Ministry for the Environment (MfE).

Benestad, R. E. (2002). Empirically downscaled temperature scenarios for northern Europe based on a multi-model ensemble. *Climate Research, 21*(2), 105-125.

Bouraoui, R., Lahmar, M., Majdoub, A., Djemali, M., & Belyea, R. (2002). The relationship of temperature-humidity index with milk production of dairy cows in a Mediterranean climate. *Animal Research, 51*(6), 479-491.

Brito-Castillo, L., Douglas, A. V., Leyva-Contreras, A., & Lluch-Belda, D. (2003). The effect of large-scale circulation on precipitation and streamflow in the Gulf of California continental watershed. *International Journal of Climatology, 23*(7), 751-768. 10.1002/joc.913

Butcher Partners Ltd. (2009). *Regional and national impacts of the 2007-2009 drought*: Prepared for MAF Policy by Butcher Partners Ltd. July 2009.

Carter, T. R., La Rovere, E. L., Jones, R. N., Leemans, R., Mearns, L. O., Nakicenovic, N., et al. (2001). Developing and Applying Scenarios. In *IPCC, 2001: Climate Change 2001: Impacts, Adaptation, and Vulnerability. CUP, Cambridge, UK.*

Chang, E. K., Guo, Y., & Xia, X. (2012). CMIP5 multimodel ensemble projection of storm track change under global warming. Journal of Geophysical Research: Atmospheres (1984–2012), 117(D23) pgs 19.

Clarke, L., J. Edmonds, H. Jacoby, H. Pitcher, J. Reilly, R. Richels, 2007. Scenarios of Greenhouse Gas Emissions and Atmospheric Concentrations. Sub-report 2.1A of Synthesis and Assessment Product 2.1 by the U.S. Climate Change Science Program and the Subcommittee on Global Change Research. Department of Energy, Office of Biological & Environmental Research, Washington, 7 DC., USA, 154 pp.

Cubasch, U., G. A. Meehl, G. J. Boer, R., J. Stouffer, M. Dix, A. Noda, et al. (2001). Projections of future climate change, in Climate Change 2001: The Scientific Basis. In E. J. T. Houghton et al. (Ed.), (pp. pp. 525-582,): Cambridge Univ. Press, New York.

Dai, A. (2006). Precipitation Characteristics in Eighteen Coupled Climate Models. *Journal of Climate, 19*(18), 4605-4630. doi:10.1175/JCLI3884.1

Dai, A., Trenberth, K. E., & Qian, T. (2004). A Global Dataset of Palmer Drought Severity Index for 1870-2002: Relationship with Soil Moisture and Effects of Surface Warming. *Journal of Hydrometeorology, 5*(6), 1117-1130.

de la Casa, A. C., & Ravelo, A. C. (2003). Assessing temperature and humidity conditions for dairy cattle in Córdoba, Argentina. *International Journal of Biometeorology, 48*(1), 6-9. 10.1007/s00484-003-0179-x

Dragovich, D. (1979). Effect of high temperature-humidity conditions on milk production of dairy herds grazed on farms in a pasture-based feed system. *International Journal of Biometeorology, 23*(1), 15-20. 10.1007/bf01553373

Emori, S., & Brown, S. J. (2005). Dynamic and thermodynamic changes in mean and extreme precipitation under changed climate. *Geophys. Res. Lett., 32*(17), L17706. 10.1029/2005gl023272

Fujino, J., R. Nair, M. Kainuma, T. Masui, Y. Matsuoka, 2006. Multi-gas mitigation analysis on stabilization scenarios using AIM global model. Multigas Mitigation and Climate Policy. The Energy Journal Special Issue.

Hahn, G. L., Gaughan, J. B., Mader, T. L., & Eigenberg, R. A. (2009). Thermal indices and their applications for livestock environments. In *Livestock Energetics and Thermal Environmental Management. Chapter 5* (pp. pp. 113-130).

Hijioka, Y., Y. Matsuoka, H. Nishimoto, M. Masui, and M. Kainuma,(2008). Global GHG emissions scenarios under GHG concentration stabilization targets. Journal of Global Environmental Engineering 13, 97-108.

Hosking, J. R. M., & Wallis, J. R. (1997).Regional Frequency Analysis: An approach based on L-Moments.

Hromadkali, T. V. (1989). The rational method in stormwater management modelling of peak flow flood control systems, I: Theoretical development. *Environmental Software, 4*(3), 123-129.

IPCC. (2000). *Emissions Scenarios. A Special Report of Working Group II of the Intergovernmental Panel on Climate Change.* Cambridge: Cambridge University Press.

IPCC. (2007a). *Climate Change 2007: The Physical Science Basis. Contribution of Working Group I to the Fourth Assessment Report of the Intergovernmental Panel on Climate Change* Cambridge, United Kingdom and New York, NY, USA.: Cambridge University Press.

IPCC. (2007b). *Climate Change 2007: Impacts, Adaptation and Vulnerability. Contribution of Working Group II to the Fourth Assessment Report of the Intergovernmental Panel on Climate Change*. Cambridge: Cambridge University Press, UK.

IPCC. (2010). *Climate Change 2010: The Physical Science Basis. Contribution of Working Group I to the Fourth Assessment Report of the Intergovernmental Panel on Climate Change* Cambridge, United Kingdom and New York, NY, USA.: Cambridge University Press.

IPCC. (2013). *Climate Change 2013: The Physical Science Basis. Contribution of Working Group I to the Fifth Assessment Report of the Intergovernmental Panel on Climate Change* Cambridge, United Kingdom and New York, NY, USA.: Cambridge University Press.

IPCC. (2014) IPCC, 2014: Summary for Policymakers. In: Climate Change 2014: Impacts, Adaptation, and Vulnerability. Part A: Global and Sectoral Aspects. Contribution of Working Group II to the Fifth Assessment Report of the Intergovernmental Panel on Climate Change [Field, C.B., V.R. Barros, D.J. Dokken, K.J. Mach, M.D. Mastrandrea, T.E. Bilir, M. Chatterjee, K.L. Ebi, Y.O. Estrada, R.C. Genova, B. Girma, E.S. Kissel, A.N. Levy, S. MacCracken, P.R. Mastrandrea, and L.L. White (eds.)]. Cambridge University Press, Cambridge, United Kingdom and New York, NY, USA, pp. 1-32.

IPCC, 2014: Climate Change 2014: Impacts, Adaptation, and Vulnerability. Part A: Global and Sectoral Aspects. Contribution of Working Group II to the Fifth Assessment Report of the Intergovernmental Panel on Climate Change [Field, C.B., V.R. Barros, D.J. Dokken, K.J. Mach, M.D. Mastrandrea, T.E. Bilir, M. Chatterjee, K.L. Ebi, Y.O. Estrada, R.C. Genova, B. Girma, E.S. Kissel, A.N. Levy, S. MacCracken, P.R. Mastrandrea, and L.L. White (eds.)]. Cambridge University Press, Cambridge, United Kingdom and New York, NY, USA, Final Draft.

Jones, R. N. (2010). *A risk management approach to climate change adaptation, in: New Zealand Climate Change Centre 2010.Climate change adaptation in New Zealand: Future scenarios and some sectoral perspectives.* , Wellington.

Kharin, V. V., Zwiers, F. W., Zhang, X., & Hegerl, G. C. (2007). Changes in Temperature and Precipitation Extremes in the IPCC Ensemble of Global Coupled Model Simulations. *Journal of Climate, 20*(8), 1419-1444. doi:10.1175/JCLI4066.1

Kharin, V.V., Zwiers, F.W., Zhang, X., Wehner, M. (2013) Changes in temperature and precipitation extremes in the CMIP5 ensemble. Climatic Change 119: 345-357

Kiktev, D., Caesar, J., Alexander, L. V., Shiogama, H., & Collier, M. (2007). Comparison of observed and multimodeled trends in annual extremes of temperature and precipitation. *Geophys. Res. Lett., 34*(10), L10702. 10.1029/2007gl029539

Kriticos, D. J., Sutherst, R. W., Brown, J. R., Adkins, S. W., & Maywald, G. F. (2003). Climate change and the potential distribution of an invasive alien plant: Acacia nilotica ssp. indica in Australia. *Journal of Applied Ecology, 40*(1), 111-124. 10.1046/j.1365-2664.2003.00777.x

Li Y., and Ye W. (2011). Applicability of ensemble pattern scaling method on precipitation intensity   indices at regional scale, Hydrology and Earth System Sciences Discussion, 8, 5227–5261, doi:10.5194/hessd-8-5227-2011.

Lu, X., & Hulme, M. (2002). A Short Note on Scaling GCM Climate Response Patterns. Prepared for the AIACC regional study teams. June 2002. http://www.aiaccproject.org/resources/GCM/GCM.html

MAF. (2009). Drought Guide: Drought definition, recognition and assistance measures. From http://www.maf.govt.nz/mafnet/rural-nz/adverse-events/droughts/drought-guide.htm

Malamud, B. D., & Turcotte, D. L. (2006). The applicability of power-law frequency statistics to floods. *Journal of Hydrology, 322*(1-4), 168-180.

Malamud, B. D., & Turcotte, D. L. (2006). The applicability of power-law frequency statistics to floods. *Journal of Hydrology, 322*(1-4), 168-180.

Mayer, D. G., Davison, T. M., McGowan, M. R., Young, B. A., Matschoss, A. L., Hall, A. B., et al. (1999). Extent and economic effect of heat loads on dairy cattle production in Australia. *Australian Veterinary Journal, 77*(12), 804-808. 10.1111/j.1751-0813.1999.tb12950.x

McMaster, G. S., & Wilhelm, W. W. (1997). Growing degree-days: one equation, two interpretations. *Agricultural and Forest Meteorology, 87*(4), 291-300.

Meehl GA, S. T., Collins WD, Friedlingstein P, Gaye AT, Gregory JM, Kitoh A, Knutti R, Murphy JM, Noda A, Raper SCB, Watterson IG, Weaver AJ and Zhao Z-C. . (2007). Global climate projections. In Climate Change 2007: The physical science basis. Contribution of Working Group I to the Fourth Assessment Report of the Intergovernmental Panel on Climate Change In S. Solomon, D. Qin, M. Manning, Z. Chen, M. Marquis, K. B. Averyt, T. M. & & M. (Eds.) (Eds.): Cambridge, UK and New York, NY: Cambridge University Press.

MfE. (2008). *Climate Change Effects and Impacts Assessment: A Guidance Manual for Local Government in New Zealand. 2nd Edition.* : Ministry for the Environment, Wellington.

MfE. (2010). *Tools for estimating the effects of climate change on flood flow: A guidance manual for local government in New Zealand*: Prepared for Ministry for the Environment.

Min, S.-K., Simonis, D., & Hense, A. (2007). Probabilistic climate change predictions applying Bayesian model averaging. *Philosophical Transactions of the Royal Society A: Mathematical, Physical and Engineering Sciences, 365*(1857), 2103-2116. 10.1098/rsta.2007.2070

Mitchell, T. D. (2001). *An investigation of the pattern scaling technique for describing future climates.*, University of East Anglia, Norwich.

Mitchell, T. D. (2003). Pattern Scaling: An Examination of the Accuracy of the Technique for Describing Future Climates. *Climatic Change, 60*(3), 217-242. 10.1023/a:1026035305597

Mullan, A. B., Wratt, D. S., & Renwick, J. A. (2001). Transient model scenarios of climate changes for New Zealand. *Weather and Climate 21* 3-43.

Mullan B, Porteous A, Wratt D, & M, H. (2005). *Changes in drought risk with climate change*: Prepared for Ministry for the Environment (NZ Climate Change Office) and Ministry of Agriculture and Forestry.

Mullan, B., & Dean, S. (2009). *AR4 climate model validation and scenarios for New Zealand. Extended Abstract*. Paper presented at the 9th International Conference on Southern Hemisphere Meteorology and Oceanography.

Mullan, B., Carey-Smith, T., Griffiths, G., Sood, A. (2011), Scenarios of storminess and regional wind extremes under climate change, prepared for Ministry of Agriculture and Forestry.

Murphy, J. M., Booth, B. B. B., Collins, M., Harris, G. R., Sexton, D. M. H., & Webb, M. J. (2007). A methodology for probabilistic predictions of regional climate change from perturbed physics ensembles. *Philosophical Transactions of the Royal Society A: Mathematical, Physical and Engineering Sciences, 365*(1857), 1993-2028. 10.1098/rsta.2007.2077

Murphy, J. M., Sexton, D. M. H., Barnett, D. N., Jones, G. S., Webb, M. J., Collins, M., et al. (2004). Quantification of modelling uncertainties in a large ensemble of climate change simulations. *Nature, 430*(7001), 768-772.

Parry, M., & Carter, T. (1998). *Climate Impact and Adaptation Assessment*. London, UK: Earthscan Publications Ltd.

Patz, J. A., Campbell-Lendrum, D., Holloway, T., & Foley, J. A. (2005). Impact of regional climate change on human health. *Nature, 438*(7066), 310-317.

Perkins, S. E., Pitman, A. J., Holbrook, N. J., & McAneney, J. (2007). Evaluation of the AR4 Climate Models Simulated Daily Maximum Temperature, Minimum Temperature, and Precipitation over Australia Using Probability Density Functions. *Journal of Climate, 20*(17), 4356-4376.

Räisänen, J. (2007). How reliable are climate models? *Tellus A, 59*(1), 2-29. 10.1111/j.1600-0870.2006.00211.x

Ramankutty, N., Foley, J. A., Norman, J., & McSweeney, K. (2002). The global distribution of cultivable lands: current patterns and sensitivity to possible climate change. *Global Ecology and Biogeography, 11*(5), 377-392. 10.1046/j.1466-822x.2002.00294.x

Raper, S. C. B., Gregory, J. M., & Osborn, T. J. (2001). Use of an upwelling-diffusion energy balance climate model to simulate and diagnose A/OGCM results. *Climate Dynamics, 17*(8), 601-613. 10.1007/pl00007931

Riahi, K. Gruebler, A. and Nakicenovic N.: 2007. Scenarios of long-term socio-economic and environmental development under climate stabilization. Technological Forecasting and Social Change 74, 7, 887-935.

Root, T. L., Price, J. T., Hall, K. R., Schneider, S. H., Rosenzweig, C., & Pounds, J. A. (2003). Fingerprints of global warming on wild animals and plants. *Nature, 421*(6918), 57-60.

Ruosteenoja, K., Tuomenvirta, H., & Jylhä, K. (2007). GCM-based regional temperature and precipitation change estimates for Europe under four SRES scenarios applying a super-ensemble pattern-scaling method. *Climatic Change, 81*(0), 193-208. 10.1007/s10584-006-9222-3

Sansom, J., & Renwick, J. A. (2007). Climate Change Scenarios for New Zealand Rainfall. *Journal of Applied Meteorology and Climatology, 46*(5), 573-590. doi:10.1175/JAM2491.1

Santer, B. D., Wigley, T. M. L., Schlesinger, M. E., & Mitchell, J. F. B. (1990). *Developing Climate Scenarios from Equilibrium GCM Results, MPI Report Number 47,* Hamburg.

Semenov, & Bengtsson. (2002). Secular trends in daily precipitation characteristics: greenhouse gas simulation with a coupled AOGCM. *Climate Dynamics, 19*(2), 123-140. 10.1007/s00382-001-0218-4

Smith, S.J. and T.M.L. Wigley, 2006. Multi-Gas Forcing Stabilization with the MiniCAM. Energy Journal (Special Issue 3) pp 373-391.

Sorteberg, A., & Kvamstø, N. G. (2006). The effect of internal variability on anthropogenic climate projections. *Tellus A, 58*(5), 565-574. 10.1111/j.1600-0870.2006.00202.x

Sutherst, R. W. (1998). Implications of global change and climate variability for vector-borne diseases: generic approaches to impact assessments. *International Journal for Parasitology, 28*(6), 935-945.

Tebaldi, C., Hayhoe, K., Arblaster, J., & Meehl, G. (2006). Going to the Extremes. *Climatic Change, 79*(3), 185-211. 10.1007/s10584-006-9051-4

Theurillat, J.-P., & Guisan, A. (2001). Potential Impact of Climate Change on Vegetation in the European Alps: A Review. *Climatic Change, 50*(1), 77-109. 10.1023/a:1010632015572

Thuiller, W., Lavorel, S., & Araújo, M. B. (2005). Niche properties and geographical extent as predictors of species sensitivity to climate change. *Global Ecology and Biogeography, 14*(4), 347-357. 10.1111/j.1466-822X.2005.00162.x

Trenberth, K. E. (1999). Conceptual Framework for Changes of Extremes of the Hydrological Cycle with Climate Change. *Climatic Change, 42*(1), 327-339. 10.1023/a:1005488920935

Van Vuuren, D., M. den Elzen, P. Lucas, B. Eickhout, B. Strengers, B. van Ruijven, S. Wonink, R. van Houdt, 2007. Stabilizing greenhouse gas concentrations at low levels: an assessment of reduction strategies and costs. Climatic Change, doi:10.1007/s/10584-006-9172-9.

Walpita-Gamage, S. H. P., Hewa, G. A., Subhashini, W. H. C., Daniell, T. M. a., & Kemp, D. (2009). *Modelling the extreme floods of South Australian catchments.* Paper presented at the 18th World IMACS Congress and MODSIM09 International Congress on Modelling and Simulation Cairns, Australia. July 2009.

Whetton, P. H., McInnes, K. L., Jones, R. N., Hennessy, K. J., Suppiah, R., Page, C. M., et al. (2005). *Australian Climate Change Projections for Impact Assessment and Policy Application: A Review.* : CSIRO Marine and Atmospheric Research, Aspendale, Victoria, Australia.
Wise, MA, KV Calvin, AM Thomson, LE Clarke, B Bond-Lamberty, RD Sands, SJ Smith, AC Janetos, JA Edmonds. 2009. Implications of Limiting CO2 Concentrations for Land Use and Energy. Science. 324:1183-1186. May 29, 2009.
Woodward, F. I. (1987). *Climate and Plant Distribution* Cambridge: Cambridge University Press.

6 Appendices

6.1 Appendix 1: Pattern Scaling Methodology

Pattern scaling is based on the theory that, firstly, a simple climate model can accurately represent the global responses of a GCM, even when the response is non-linear (Raper et al., 2001), and secondly, a wide range of climatic variables represented by a GCM are a linear function of the global annual mean temperature change represented by the same GCM at different spatial and/or temporal scales (Mitchell, 2003; Whetton et al., 2005). Scaling local trends by projections of global warming and comparing these to model projections will allow adaptation needs at the local and regional scale to be assessed. For example, pattern-scaled historical data can be compared with pattern scaling from GCMs.

Pattern scaling involves the following general steps (Lu and Hulme, 2002):

Step 1: Defining the 'master pattern' – a single GCM experiment run (or ideally an ensemble) with a corresponding RCP emissions scenario pattern for one climate variable, such as global mean temperature;

Step 2: Normalising the 'master pattern' - the climate change values for each individual grid cell in the 'master pattern' are normalised by subtracting the 'average' value for the global mean temperature (for that GCM experiment run) from each grid cell. This normalised pattern then represents the degree of warming in each grid cell, per degree global warming;

Step 3: Obtaining scalars – this derives the global warming values per grid cell in a climate pattern, for a time in the future for a given emissions scenario, simulated by a simple climate model such as MAGICC SCENGEN;

Step 4: Scaling the normalised pattern – the pattern of changes for the future time period can be produced by multiplying the normalised pattern in Step 2 by the respective scalar developed in Step 3.

Pattern scaling may be described as follows: for a given climate variable *V*, its anomaly ΔV^* for a particular grid cell (*i*), month (*j*) and year or period (*y*) under an emission forcing scenario SRES A1B:

$$\Delta V^*_{yij} = \Delta T_y \cdot \Delta V'_{ij} \qquad (1)$$

ΔT being the annual global mean temperature change.

The local change pattern value ($\Delta V_{ij}^{'}$) was calculated from the GCM simulation anomaly (ΔV_{yij}) using linear least squares regression, that is, the slope of the fitted linear line.

$$\Delta V_{ij}^{'} = \frac{\sum_{y=1}^{m} \Delta T_y \cdot \Delta V_{yij}}{\sum_{y=1}^{m} (\Delta T_y)^2} \qquad (2)$$

where *m* is the number of future sample periods used, with a 10 year average as a period.

Pattern-scaling does not seem to be a very large source of error in constructing regional climate projections, even for extreme scenarios (Ruosteenoja et al., 2007). However, in applying pattern-scaling, two fundamental sources of error related to its underlying theory need to be addressed: 1) the non-linearity error: the local responses of climate variables, precipitation in particular, may not be inherently linear functions of the global mean temperature change; and 2) noise due to the internal variability of the GCM. Based on the pattern scaling theory, for a given GCM, the linear response change pattern of a climate variable to global mean temperature change represented by the GCM should be obtained from any one of its GHG emission simulation outputs.

Table 10 provides a list of GCMs used in this analysis.

Table 11 GCMs used in SimCLIM climate variable patterns.

	Model	Country	Spatial resolution for atmospheric variable (longitude*latitude)	Spatial resolution for ocean variable (longitude*latitude)
1	ACCESS1.3	Australia	192*145	360*300
2	ACCESS1.0	Australia	192*145	360*300
3	BCC-CSM1-1	China	128*64	360*232
4	BCC-CSM1-1-m	China	320*160	360*232
5	BNU-ESM	China	128*64	
6	CanESM2	Canada	128*64	256*192
7	CCSM4	USA	288*192	320*384
8	CESM1-BGC	USA	288*192	320*384
9	CESM1-CAM5	USA	288*192	320*384
10	CMCC-CM	Italy	480*240	182*149
11	CMCC-CMS	Italy	192*96	182*149
12	CNRM-CM5	France	256*128	362*292
13	CSIRO-Mk3-6-0	Australia	192*96	192*189
14	EC-EARTH	Netherlands	320*160	362*292
15	FGOALS-g2	China	128*60	360*196
16	FGOALS-s2	China	128*108	360*196
17	GFDL-CM3	USA	144*90	360*200
18	GFDL-ESM2G	USA	144*90	360*210
19	GFDL-ESM2M	USA	144*90	360*200
20	GISS-E2-H	USA	144*90	144*90
21	GISS-E2-H-CC	USA	144*90	144*90
22	GISS-E2-R	USA	144*90	288*180
23	GISS-E2-R-CC	USA	144*90	288*180
24	HADCM3	UK	96*73	96*73
25	HadGEM2-AO	UK	192*145	360*216
26	HadGEM2-CC	UK	192*145	360*216
27	HadGEM2-ES	UK	192*145	360*216
28	INMCM4	Russia	180*120	360*340
29	IPSL-CM5A-LR	France	96*96	182*149
30	IPSL-CM5A-MR	France	144*142	182*149
31	IPSL-CM5B-LR	France	96*96	182*149
32	MIROC4H	Japan	640*320	1280*912
33	MIROC5	Japan	256*128	256*224
34	MIROC-ESM	Japan	128*64	256*192
35	MIROC-ESM-CHEM	Japan	128*64	256*192
36	MPI-ESM-LR	Germany	192*96	256*220
37	MPI-ESM-MR	Norway	192*96	802*404
38	MRI-CGCM3	Japan	320*160	360*368
39	NorESM1-M	Norway	144*96	320*384
40	NorESM1-ME	Norway	144*96	320*384

Table 12 Availability of GCM variables in SImCLIM 2013 Waikato data package

	Model	Tmean	Tmax	Tmin	Precip	SolRad	SLR	GEV
1	ACCESS1.3	√	√	√	√	√	√	√
2	ACCESS1.0	√	√	√	√	√	√	
3	BCC-CSM1-1	√	√	√	√		√	
4	BCC-CSM1-1-m	√	√	√	√		√	
5	BNU-ESM	√	√	√	√			
6	CanESM2	√	√	√	√	√	√	√
7	CCSM4	√	√	√	√	√	√	√
8	CESM1-BGC	√	√	√	√	√		√
9	CESM1-CAM5	√	√	√	√	√		
10	CMCC-CM	√	√	√	√	√	√	√
11	CMCC-CMS	√	√	√	√	√	√	√
12	CNRM-CM5	√	√	√	√	√	√	√
13	CSIRO-Mk3-6-0	√	√	√	√	√	√	√
14	EC-EARTH	√	√	√	√			
15	FGOALS-g2	√	√	√	√			
16	FGOALS-s2	√	√	√	√			
17	GFDL-CM3	√	√	√	√	√	√	
18	GFDL-ESM2G	√	√	√	√	√	√	√
19	GFDL-ESM2M	√	√	√	√	√	√	√
20	GISS-E2-H	√	√	√	√	√		
21	GISS-E2-H-CC	√	√	√	√	√		
22	GISS-E2-R	√	√	√	√	√	√	
23	GISS-E2-R-CC	√	√	√	√	√	√	
24	HADCM3	√	√	√	√	√		
25	HadGEM2-AO	√	√	√	√	√		
26	HadGEM2-CC	√	√	√	√	√	√	
27	HadGEM2-ES	√	√	√	√	√	√	√
28	INMCM4	√	√	√	√	√	√	√
29	IPSL-CM5A-LR	√	√	√	√	√	√	√
30	IPSL-CM5A-MR	√	√	√	√	√	√	√
31	IPSL-CM5B-LR	√	√	√	√	√		√
32	MIROC4H	√	√	√	√	√		
33	MIROC5	√	√	√	√	√	√	√
34	MIROC-ESM	√	√	√	√	√	√	√
35	MIROC-ESM-CHEM	√	√	√	√	√	√	√
36	MPI-ESM-LR	√	√	√	√	√	√	√
37	MPI-ESM-MR	√	√	√	√	√	√	√
38	MRI-CGCM3	√	√	√	√	√	√	√
39	NorESM1-M	√	√	√	√		√	√
40	NorESM1-ME	√	√	√	√		√	

6.2 Appendix 2: RCP Scenarios (IPCC, 2013)

The Representative Concentration Pathways (RCPs) are four greenhouse gas concentration (not emissions) trajectories adopted by the IPCC for its Fifth Assessment Report (AR5). The four RCPs, RCP2.6, RCP4.5, RCP6.0, and RCP8.5, are named after a possible range of radiative forcing values in the year 2100 (of 2.6, 4.5, 6.0, and 8.5 W/m2, respectively).

RCP2.6

The RCP 2.6 is developed by the IMAGE modeling team of the Netherlands Environmental Assessment Agency. The emission pathway is representative for scenarios in the literature leading to very low greenhouse gas concentration levels. It is a so-called "peak" scenario: its radiative forcing level first reaches a value around 3.1 W/m2 mid-century, returning to 2.6 W/m2 by 2100. In order to reach such radiative forcing levels, greenhouse gas emissions (and indirectly emissions of air pollutants) are reduced substantially over time. The final RCP is based on the publication by Van Vuuren et al. (2007).

RCP4.5

The RCP 4.5 is developed by the MiniCAM modeling team at the Pacific Northwest National Laboratory's Joint Global Change Research Institute (JGCRI). It is a stabilization scenario where total radiative forcing is stabilized before 2100 by employment of a range of technologies and strategies for reducing greenhouse gas emissions. The scenario drivers and technology options are detailed in Clarke et al. (2007). Additional detail on the simulation of land use and terrestrial carbon emissions is given by Wise et al (2009).

RCP6.0

The RCP 6.0 is developed by the AIM modeling team at the National Institute for Environmental Studies (NIES), Japan. It is a stabilization scenario where total radiative forcing is stabilized after 2100 without overshoot by employment of a range of technologies and strategies for reducing greenhouse gas emissions. The details of the scenario are described in Fujino et al. (2006) and Hijioka et al. (2008).

RCP8.5

The RCP 8.5 is developed by the MESSAGE modeling team and the IIASA Integrated Assessment Framework at the International Institute for Applies Systems Analysis (IIASA), Austria. The RCP 8.5 is characterized by increasing greenhouse gas emissions over time representative for scenarios in the literature leading to high greenhouse gas concentration levels. The underlying scenario drivers and resulting development path are based on the A2r scenario detailed in Riahi et al. (2007).

6.3 Appendix 3: Methodology for extreme precipitation event analysis based on daily GCM data

This is based on the paper by Li and Ye(2011).

GCM outputs are still the most reliable source of information for future climate scenario projections. With more and more detailed GCM data becoming publicly available, including daily time series, it is now possible to pursue more advanced methods for daily extreme precipitation event analysis, which can be based on the finer temporal results. GCMs have relatively poor performance on simulating precipitation at a regional or local scale compared to the historical observed data. This has seriously limited the direct use of GCM precipitation time series in extreme precipitation event analysis. Dynamic downscaling improves the accuracy at finer scales but only to a limited extent. A major drawback of this method is its high computational demand for only one or two simulation outputs. This makes it very difficult for uncertainty analysis for different emission scenarios and different GCMs. A statistical downscaling technique provides a computationally efficient and hence cost-effective solution that can lead to improved accuracy of GCM results. The results can be used not only in the generation of precipitation time series, but also for the analysis of the possible changes to extreme precipitation events under different climate change scenarios. To date, scientific research has not produced a satisfactory method at a fine spatial scale that readily can be implemented for simulating daily precipitation, particularly for extreme analysis.

Among the wide range of climate variables, precipitation extremes have attracted much research attention because of the potential disasters these may cause to human society and natural systems. Extreme precipitation events are projected to increase with climate change, even in areas where the total precipitation is projected to decrease (Meehl et al., 2007), since global warming will noticeably enhance the hydrological cycle at both global and local scales. In order to adequately assess the climate change impact on extreme precipitation events, the characteristics of GCM-simulated precipitation and its relationship with global warming need to be evaluated (Perkins et al., 2007; Alexandra and Arblaster, 2008). The evaluation of observed and modeled trends has shown that the confidence in GCM projected extremes of precipitation is much less than that of temperature (e.g. Kharin et al., 2007; Kiktev et al., 2007). In general, the magnitude of changes in precipitation extremes simulated by GCMs was found to have a linear relationship with the strength of GHG emissions or in proportion with the global warming trend (Alexander and Arblaster, 2009, Tebaldi et al., 2006), which is in alignment with the linear response theory of pattern scaling.

On the other hand, given the current state of scientific understanding and the limitations of GCMs in simulating the complex climate system, a large ensemble of GCM simulations is more appropriate in climate change projections than using individual GCM simulation outputs, particularly if such projections will be used for impact assessments, because only large ensembles of GCM simulations, sampling the widest possible range of modelling uncertainties, can provide a reliable specification of the spread of possible regional changes (Murphy et al., 2004; Sorteberg and Kvamstø, 2006; Murphy et al., 2007; Räisänen, 2007).

Simulations of extreme precipitation in GCMs cannot be expected to accurately reproduce observed absolute quantities or rates of change. The relatively coarse resolution of GCMs prevents the simulation of phenomena that manifest their intensity mainly at synoptic (i.e., regional) scales (Dai, 2006; Tebaldi et al., 2006). GCM-simulated extreme precipitation intensities are systemically much lower than the observed data (Dai, 2006; Kharin et al., 2007).

In lieu of the above, we present the following method for analysing the climate change impact on extreme precipitation using daily GCM outputs at their original spatial resolution (i.e. not downscaled) (Li and Ye, 2009). The steps of this method are listed below:

1. Build a General Extreme Value (GEV) distribution for one GCM baseline period (1986-2005) for daily data and calculate its extreme precipitation intensity values for 11 selected return periods (5 ,10, 20,30,50,100,150,200,300 year periods);

2. Build GEV distribution for the above GCM based on its future daily data. There are 16 20-year periods from 2006-2025 to 2081-2100 for 2 RCP scenarios RCP4.5 and RCP8.5 available from the IPCC AR5 data archive.

3. Calculate the extreme precipitation intensity values for the 11 selected return periods as baseline period;

4. Calculate the difference in percentage of the extreme precipitation intensity values between baseline and each future period;

5. Calculate the annual global average mean temperature change between the future periods and the baseline for the above GCM;

6. Normalise the extreme precipitation changes by the linear least square regression method using the following equation:

$$\Delta V_{ij}^{'} = \frac{\sum_{y=1}^{m} \Delta T_y \cdot \Delta V_{yij}}{\sum_{y=1}^{m} (\Delta T_y)^2}$$

where $\Delta V_{ij}^{'}$ is the normalised change value for the grid cell(*i*) and return period (*j*); ΔV_{yij} is the change percentage for ΔT_y for global mean temperature change for the future period *y*; *m* =6, the number of future sample periods used.

With the use of bi-linear interpolation, a finer-scale change pattern of extreme precipitation is obtained at the required spatial resolution (example in Figure XXXX).

By applying the change pattern generated from daily GCM data, it is possible to undertake an extreme precipitation event analysis for the Waikato region.

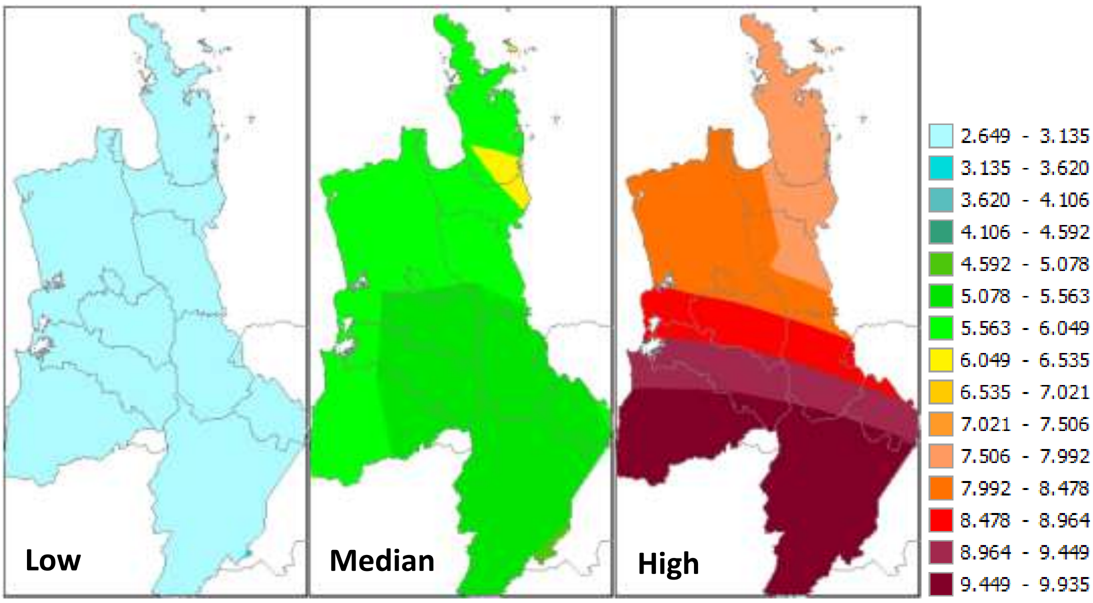

Figure 25 Sample of extreme precipitation change patterns (%) for ARI = 50 years. From left to right, panels show the 25th, Median, and 75th percentile values of 22 GCMs.

7. Build GEV distribution from historical gridded daily data of the Waikato region and calculate the extreme precipitation values for the selected return period (10, 20, 50, 100, and 200 years) ;
8. Extract the change pattern values from global change patterns generated in step 6 above;
9. Obtain the global average mean temperature change for the selected study time slices (2030, 2070, and 2100) and RCP scenarios (RCP4.5 and RCP8.5) in mid climate sensitivity using the SimCLIM software.
10. Calculate the extreme precipitation values by manipulating the change patterns with global mean temperature using the following equation:

$$P_1 = P_0 \cdot (1 + \Delta P / 100 \times \Delta GMT_1)$$

Where, P_1 and P_0 are the future and baseline extreme precipitations, respectively; ΔP is the change percentage generated from GCM data; and *ΔGMT* (the scalar) is the change of global mean temperature increase in a future time slice.

In summary, this method can be viewed as an extension of the pattern scaling method to extreme event analysis. Preliminary work using the method for New Zealand and Australia extreme rainfall analysis has generated improved results that conform to other scientific research findings.

Limitations and future development

No statistical downscaling method was involved in this method. Daily GCM precipitation outputs were analyzed in their original spatial resolution in order to retain the extreme precipitation change trend of GCMs. A statistical downscaling method is under development by Climsystems Ltd, which is expected to reflect the extreme precipitation change trend of GCMs in higher spatial resolution with more local information.

MfE (2008) provided a table for extreme precipitation change against global warming. This table recommends that *percentage* adjustments are applied to extreme rainfall per 1 degree Celsius of warming, for a range of ARIs or return periods for the duration of 10 minutes to 72 hours. The entries for the 10-minute duration are based on the theoretical increase in the amount of water held in the atmosphere for a 1 degree increase in temperature (8%). Entries for other durations are based on logarithmic (in time) interpolation between the 10-minute and 24-hour rates.

Table 12 provides the list of GCMs used for this analysis.

Table 9 GCMs used in SimCLIM extreme precipitation analysis

	Model	Country	Spatial resolution for atmospheric variable (longitude*latitude)	Spatial resolution for ocean variable (longitude*latitude)
1	ACCESS1.3	Australia	192*145	360*300
2	CanESM2	Canada	128*64	256*192
3	CCSM4	USA	288*192	320*384
4	CESM1-BGC	USA	288*192	320*384
5	CMCC-CM	Italy	480*240	182*149
6	CMCC-CMS	Italy	192*96	182*149

7	CNRM-CM5	France	256*128	362*292
8	CSIRO-Mk3-6-0	Australia	192*96	192*189
9	GFDL-ESM2G	USA	144*90	360*210
10	GFDL-ESM2M	USA	144*90	360*200
11	HadGEM2-ES	UK	192*145	360*216
12	INMCM4	Russia	180*120	360*340
13	IPSL-CM5A-LR	France	96*96	182*149
14	IPSL-CM5A-MR	France	144*142	182*149
15	IPSL-CM5B-LR	France	96*96	182*149
16	MIROC5	Japan	256*128	256*224
17	MIROC-ESM	Japan	128*64	256*192
18	MIROC-ESM-CHEM	Japan	128*64	256*192
19	MPI-ESM-LR	Germany	192*96	256*220
20	MPI-ESM-MR	Norway	192*96	802*404
21	MRI-CGCM3	Japan	320*160	360*368
22	NorESM1-M	Norway	144*96	320*384

6.4 Appendix 4: Computation of the Potential Evapotranspiration Deficit, PED

The water balance calculation used to derive the Potential Evapotranspiration Deficit (*PED*) index assumes that the water gains and losses to the soil profile are typically in balance (Mullan et al., 2005). Provided that water is non-limiting, the balance for a given rainfall period can be written as:

$P = PET + Ro + D \pm \Delta S$

Where *P* is precipitation, *PET* is potential (or upper limit) evapotranspiration, *Ro* is surface runoff, *D* is drainage loss through percolation, and ΔS is the change in water storage. For the purposes of this study, *PET* is calibrated for pasture water use.

In principle, for each day,

$S = S_{d-1} + P - PET - Ro - D$

Where *S* is the new storage, and S_{d-1} is the water storage for the previous day.

Field capacity water storage is defined by the Available Water Capacity *(AWC)*, which was taken to be 150 mm for this study (Mullan et al., 2005). Rainfall in excess of field capacity is assumed to be lost to the water balance by runoff and drainage.

if $\quad S_{d-1} + P - PET > AWC$

then $\quad (S_{d-1} + P - PET) - AWC = (Ro + D)$

As *S* is reduced, it becomes increasingly difficult for plants to extract water from the soil, and water transpiration decreases. Here we have used a method for estimating constrained water use by assuming evapotranspiration (ET) continues at its potential rate until half *AWC* is depleted, following which it ceases until further rain occurs.

if $\quad S < ½(AWC)$

then $\quad ET = 0$

The difference between the subsequent soil water-restricted evapotranspiration, *(RET),* and the atmospheric potential evapotranspiration for the period *(PET)*, is referred to here as the potential evapotranspiration deficit *(PED)* and is incremented on a daily basis.

$PED = PED_{d-1} + (PET - RET)$

In effect, *PED* is approximately equivalent to the amount of water that would need to be added by rainfall or irrigation to keep pasture growing at its daily potential rate.

PED was accumulated daily for the July to June year, beginning from zero each year. Note that the soil moisture deficit carries over from one year to the next, even though *PED* is reset at the beginning of each July-June period. The water balance calculation was initiated on 1 January 1976, so there was a potentially non-zero starting value of soil moisture deficit at the beginning of July 1976.

6.5 Appendix 5: Calculation of the Temperature Humidity Index (THI)

The Temperature Humidity Index (THI) was calculated using the following equation (Mayer et al., 1999):

$$THI = T + 0.36T_d + 41.2$$

Where, T is air temperature (degrees Celsius) and T_d is the dew point temperature (°C) which was calculated as follows:

$$T_d = \frac{b\gamma(T,RH)}{a - \gamma(T,RH)}$$

Where

$$\gamma(T,RH) = \frac{aT}{b+T} + \ln(RH/100)$$

Where the temperatures are in degrees Celsius (°C) and, *ln* refers to the natural logarithm, RH refers to relative humidity.

The constants are:

a = 17.271, b = 237.7 °C

The hourly temperature T was calculated from the daily maximum and minimum temperature using the method by De Wit et al., 1978. Temperature data were divided into two sets: from sunrise to 1400h and from 1400 to sunrise hour. The method assumes *Tmax* at 1400 and *Tmin* at sunrise. Therefore, the temperature for hour *h* was calculated using the following equations:

$T(h) = TAVE - AMP(\cos(\pi(h - RISE)/(14 - RISE)))$, if h>RISE and h<=14

$T(h) = TAVE + AMP(\cos(\pi(h - 14)/(RISE - 14)))$, for other hours

Where, *h* is the local hour of a day (0100-2400), RISE is the sunrise hour, TAVE and AMP are defined as:

TAVE= (TMAX+TMIN)/2.0, AMP = (TMAX-TMIN)/2.0

The average temperature of the hottest 3 hours in each day was used for the THI calculation.